Title

THE SURFACE STRUCTURE AND BONDING OF (2X2) ACETYLENE OVERLAYERS ON PLATINUM (111): LEED INTENSITY ANALYSIS

Author

Kesmodei, L.L.

Publication Date

1977-02-01

Submitted to Journal of Chemical Physics

LBL-5407 Rev.
Preprint

THE SURFACE STRUCTURE AND BONDING OF (2X2) ACETYLENE OVERLAYERS ON PLATINUM (111): LEED INTENSITY ANALYSIS

L. L. Kesmodel, R. C. Baetzold, and G. A. Somorjai

February 18, 1977

Prepared for the U. S. Energy Research and Development Administration under Contract W-7405-ENG-48

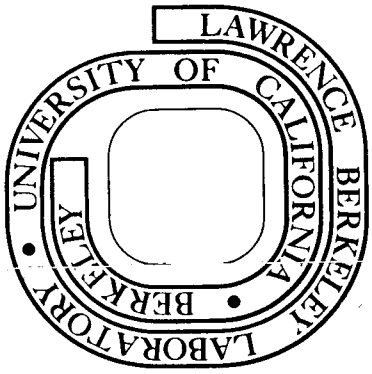

LBL-5407 Rev.

DISCLAIMER

LBL 5407 Rev

THE SURFACE STRUCTURE AND BONDING OF (2X2) ACETYLENE OVERLAYERS ON PLATINUM (111): LEED INTENSITY ANALYSIS

by

L. L. Kesmodel, R. C. Baetzold* and G. A. Somorjai

Materials and Molecular Research Division, Lawrence Berkeley Laboratory
and Department of Chemistry, University of California,
Berkeley, California 94720

ABSTRACT

We report the results of a low-energy electron diffraction intensity analysis of the structure of (2x2) arrays of acetylene (C_2H_2) on the Pt(111) surface. We have determined the structure of two different bonding states of the chemisorbed species (separated by a thermal activation barrier) which were recently identified by LEED and ultraviolet photoelectron spectroscopy. The more weakly bound (metastable) state involves coordination to basically one surface metal atom (Pt-C bond lengths of 2.5(1) Å) whereas attachment to three metal atoms is found for the more strongly bound (stable) state (Pt-C bond lengths of 2.2(1) Å and 2.6(1) Å). A lack of sensitivity to possible C-C bond elongation and CCH angle-bending for the adsorbed molecule is also reported and discussed.

---

* Permanent address: Eastman Kodak Laboratories, Rochester, New York 14602.

I. INTRODUCTION

The unsaturated hydrocarbon acetylene (C_2H_2) has been observed by low-energy electron diffraction (LEED)[1] and subsequently ultraviolet photoelectron spectroscopy (UPS)[2,3] to adsorb on the platinum (111) surface in (at least) two different undissociated chemisorption states (referred to here as "metastable" and "stable") which are separated by a thermal activation barrier. In the first study of molecular chemisorption by LEED intensity-voltage (I-V) analysis,[4] we reported on our initial findings concerning the stereochemistry of the stable adsorption state which is formed (irreversibly) by heating the room-temperature metastable state to T~350 K.[1,3] (Fragmentation of C_2H_2 occurs only above T~450 K.) In the method we employed, which has been rather widely applied to clean crystalline surfaces and atomic adsorbates, the surface geometry is determined by analysis of the beam intensities of slow electrons ($10 \lesssim E \lesssim 200$ eV) diffracted from the surfaces of well-ordered systems under ultra-high vacuum conditions.[5] We found that an acetylene attachment to three surface metal atoms is favored for the stable state;[4] significantly, a similar configuration is commonly found in trinuclear metal-alkyne complexes[6] and there involves "σ" bonds to two of the metal atoms and a "π" bond to the third metal atom.[7] We ruled out, in the course of our analysis, the "di-σ" mode of attachment to two metal atoms, a configuration which has received considerable attention in the catalysis literature,[8] as well as in semi-empirical, molecular-orbital calculations.[9]

In recent UPS studies Demuth and Lo et al. have used acetylene-induced spectral features to identify activated metastable-stable C_2H_2 transitions on Pt(111)[2,3] and Pd(111)[2] surfaces. Lo et al. also found

that ethylene (C_2H_4) exhibits a room-temperature UPS spectrum ($h\nu$= 21.2 eV) on Pt(111) which is virtually identical to that of the stable acetylene species, indicating dehydrogenation ($C_2H_4 \rightarrow C_2H_2+2H$) as suggested earlier by the LEED experiments of Stair and Somorjai.[1] Demuth has proposed an interpretation of the UPS spectra in terms of a transition from a "π-bonded" species to an "olefinic" species, basing his conclusions primarily on the similarity of the photoemission difference spectrum at $h\nu$= 40.8 eV for stable acetylene to that of associatively chemisorbed ethylene (T~80 K).[2] It seems likely to us that the olefinic species identified by Demuth corresponds to the stable species we identified by LEED analysis as involving attachment to three metal atoms at approximately covalent C-Pt distances.[4] This correspondence remains uncertain, however, since the formation temperature of the stable species analyzed at this laboratory[1,3,4] differs from that reported by Demuth.[2]

In the present paper we report extensive results of a dynamical LEED I-V analysis of the Pt(111)-C_2H_2 system. We elaborate on and further justify our initial results dealing with the stable C_2H_2 state,[4] and we also identify the surface structure of the metastable state. The main results of this study as detailed in the later sections are as follows: (i) the metastable state involves coordination of C_2H_2 to essentially one Pt surface atom at a z-distance of 2.45±0.10 Å above the topmost plane of Pt atoms (a C-Pt bond length of 2.53 Å), (ii) the bonding site for the stable state is a triangular position at a z-distance of 1.95±0.10 Å (C-Pt bond lengths of 2.25 Å and 2.59 Å) and (iii) very limited sensitivity is found to either CC bond length or CCH bond angle variations, and hence no conclusions are reported here concerning these structural properties.

The metastable-stable transition thus involves sizeable contraction in C-Pt bond lengths but more importantly a change in coordination from one metal atom to three metal atoms. This observed change in coordination is likely accompanied by a change from a basically π-bonded species to a more strongly bound σ-bonded acetylene.

In Sec. II below a brief overview of pertinent acetylene-metal bonding and structures in organometallic clusters is presented. We describe in Sec. III the various aspects of the intensity analysis. The main results are presented in Sec. IV, and conclusions are summarized in Sec. V. In the Appendix, sensitivity of the calculated I-V profiles to important structural and non-structural parameters is examined.

II. MODELS OF ACETYLENE CHEMISORPTION: STEREOCHEMISTRY

The disposition and chemical state of unsaturated hydrocarbons on transition-metal surfaces has for many years been an unresolved problem of considerable interest in the fields of adsorption, adhesion and heterogeneous catalysis.[8] Competing models involving the formation of π complexes and σ complexes have been postulated for acetylene and ethylene chemisorption.[8] Generalizations of these models are also expected to apply to other unsaturated hydrocarbons on metal surfaces. In the present study of acetylene chemisorption on platinum we examine these various modes of bonding in the context of the high-symmetry bonding sites available on the (111) face of an f.c.c. crystal.

As illustrated in Fig. 1 we distinguish four sites designated as (a) π complex or the "atop" site, (b) μ-bridging, (c) di-σ and (d) triangular. These surface sites are labeled in this way to draw attention to the interesting stereochemical analogy between these surface configurations and known modes of attachment of acetylenic ligands to small transition metal clusters.[10] (We refer to ligands of the type RC≡CR where the radical R (=C_6H_5, CH_3, etc.) substitutes for H.) In Fig. 1 we schematically indicate the types of bonds found in clusters of 1-3 metal atoms and their parallel association with the particular surface sites of interest.

The one-coordinate π complex (a) is associated with attachment of an acetylene to a single transition-metal atom, and the nature of this bond in clusters is described by a model originally developed by Dewar[11] for metal-olefin bonding. In this model, the doubly occupied π_u orbital transfers electron density to a metal hybrid orbital and this transfer of charge is offset by formation of a bona fide π symmetry bond through the overlap

of a filled d_π orbital of the metal and an empty antibonding π_g orbital of the acetylene. A similar scheme has been adopted for the μ-bridging configuration (b) (favored in binuclear complexes) in which each of the two perpendicular π_u orbitals is directed towards a different metal atom thereby forming two orthogonal "μ" bonds.[12]

The geometries illustrated in Fig. 1(c) and Fig. 1(d) are generally associated in clusters with rehybridization of the acetylene to an olefinic bonding (as indicated schematically) on the basis of stereochemical data (i.e., CC bond length, CCR angles, as well as the orientation of the acetylene to the metal atoms). The di-σ geometry (c) involves the formation of two carbon-metal σ bonds and has received considerable discussion in the catalysis literature as a probable surface complex,[8] although its occurrence in organometallic clusters is uncommon. The triangular geometry (d) is thought to involve formation of two carbon-metal σ bonds as well but with an additional μ bond derived from the π framework to the unique metal atom.[6] Hence, in the triangular geometry each (equivalent) carbon atom has significant interaction with two metal atoms. This arrangement is commonly found in trinuclear metal-alkyne complexes.

In Table I we cite various organometallic compounds exhibiting the four basic surface geometries we have considered. One finds that with few exceptions all of the known clusters exhibit considerable C_2R_2 "distortions" from the gas-phase configuration in terms of CC bond length expansion and CCR angle bending.[6] For the various mononuclear metal-alkyne complexes associated with geometry (a) an average (taken over several clusters) CC length of 1.29 Å and a CCR angle of ~145° are found

compared to gas phase values of 1.20 Å and 180°. Binuclear clusters of the μ-bridging kind exhibit average CC lengths of 1.36 Å and CCR angles of ~134°. There seems to be no systematic difference in the distortions found in the binuclear and trinuclear clusters, the CC length seemingly stabilizing around 1.4 Å for the compounds thus far analyzed.

The extent of the C-C bond elongation and changes in CCH bond angles for surface adsorbed C_2H_2 species as well as other hydrocarbons with respect to their gas phase structures remains an open question presently under investigation by various surface spectroscopies. It is probable that C-C bond stretching and possibly bond scission occurs with low activation energy on some transition-metal surfaces. Both Pd(111) and Pt(111) exhibit two different chemisorption states of C_2H_2 corresponding to different stereochemistry which is likely related to changes in C-C bond order.[1-3] On the other hand, UPS data indicates the distortion on Ni(111) at 300 K to be very small.[13]

Let us note that we have examined in this work only those acetylene structures having the C-C axis parallel to the Pt surface. We consider it unlikely that large deviations from in-plane C-C orientation (without accompanying hydrogen migration) would occur for chemisorbed acetylene as it leads to minimum overlap of bonding molecular orbitals. The possibility of dissociation of acetylene at T~300-400 K to adsorbed CC, CH, CH_2 or C_2H radicals also seems improbable in view of the recent UPS studies.[2,3]

III. INTENSITY CALCULATIONS

In this section we outline the calculational procedure for obtaining the reflected beam intensities for low-energy electron diffraction given a model geometry. In recent years the quantum-mechanical methods for treating the multiple-scattering of slow electrons from crystalline surfaces have become fairly standardized; we refer the reader to reviews on the subject for details of the LEED multiple-scattering theory.[14] Here we mention only the most important features of the calculation and some specific aspects pertaining to the scattering from an acetylene molecule.

Multiple-Scattering Method: General Features

An accurate description of the I-V profiles requires the consideration of several orders of (elastic) multiple-scattering of the electrons from the attractive (screened) Coulomb fields of the atomic nuclei, which by virtue of their periodic lattice arrangement and the wave-like behavior of the electrons ($\lambda=h/\sqrt{2mE}$) give rise to diffraction effects.

In virtually all calculations the muffin-tin model[15] is employed, i.e., the scattering potential is taken to be spherically symmetric in the neighborhood of each atomic center and to be approximately constant in the interstitial region between muffin-tins. The assumption of sphericity, though inadequate for the general problem of valence electron behavior, is quite a good approximation at LEED energies: that is, in order to undergo back-scattering the LEED electron must experience the strong forces of the core-region of the atomic potential where the charge distribution is indeed spherically symmetric.

The scattering from the spherically symmetric atomic sites is given

by the conventional partial wave expansion[16] in terms of the phase shifts, δ_ℓ,

$$f(\theta) = \frac{1}{k} \sum_{\ell=0}^{\infty} (2\ell+1) e^{i\delta_\ell(k)} \sin\delta_\ell(k) P_\ell(\cos\theta) \qquad (1)$$

where $k = (2mE/\hbar^2)^{1/2}$ and P_ℓ are the Legendre polynomials. The atomic scattering factor $f(\theta)$ describes the amplitude and phase dependence of a scattering event on the scattering angle θ from the forward direction.

The mathematical formulation of multiple-scattering processes involves essentially the products of single-scattering events given by Eq. (1) with the intermediate process of electron propagation. Due to efficient loss processes in the solid such as plasmon excitation, the mean free path λ_{ee} for the occurrence of an inelastic event is ~4-8 Å at LEED energies (20-200 eV). Since these large energy loss events (ΔE~10 eV) remove electrons from the observed elastic beams, we note that the electron propagation between scattering events is a highly-damped process. This electron beam attenuation is commonly treated as being isotropic and is described in terms of λ_{ee} or equivalently in terms of an imaginary contribution (Σ_i~3 eV) to the scattering potential.

The main physical features of the calculation, then, are the elastic events parameterized by the phase shifts δ_ℓ (which are derived from the potential $V(r)$ associated with each atomic site) and inelastic damping parameterized by Σ_i. Multiple scattering formulae essentially involve these parameters in various lattice summations. In particular, we have employed a beam representation and the layer doubling method.[17]

Finally, we note that we have used the "no-reflection" treatment of the barrier between vacuum and the solid surface; that is, we consider the

barrier to smoothly accelerate the incident electron in the direction normal to the surface and neglect reflections from the barrier itself. This approximation is valid for energies greater than about 30 eV.[18]

Scattering of Low-Energy Electrons from Platinum

The parameters describing the platinum scattering were the same as those used previously[19] with the exception of the electron damping Σ_i which was taken to be 2.5 eV in this work rather than the value of 4 eV used previously. The value of 2.5 eV gives a better description of fine structure in the I-V profiles for both the clean Pt[20] and Pt-C_2H_2 systems. The value of the constant potential between muffin-tin spheres (muffin-tin zero) was V_o = 14.3 eV below the vacuum level.[19] We have neglected the decrease in work function ($\Delta\phi$ = 1.5 eV) associated with acetylene adsorption. The platinum phase shifts (Ref. 19, Fig. 1) were derived from the band-structure potential used by Andersen and Mackintosh[21] for which the exchange contribution was given by the Slater formula.[22] (Eq. (3) below.)

Scattering of Low-Energy Electrons from Acetylene

Applying the muffin-tin model to acetylene, we consider spheres centered on each of the carbon and hydrogen atoms. Within these atomic spheres a spherical average of the potential is performed; the region outside the spheres (intermolecular) has a volume average ("inner potential") which in most of the reported calculations was assumed equal to the platinum value V_o = 14.3 eV. We have in addition carried out calculations (see Appendix) in which the acetylene layer has a different inner potential from the platinum value, and we do not observe sensitivity to sizeable (5 eV) differences in potential levels even at very low electron energies.

The electronic charge density in the molecule was calculated using molecular-orbital wave functions given by Palke and Lipscomb[23] in a self-consistent field treatment with a minimal basis set of Slater atomic orbitals. The electrostatic contribution to the potential energy was calculated from Poisson's integral

$$\Phi(\underset{\sim}{r}) = \int \frac{\rho(\underset{\sim}{r}')\, d^3r'}{|\underset{\sim}{r}-\underset{\sim}{r}'|} \qquad (2)$$

employing the molecular charge density $\rho(\underset{\sim}{r})$ consisting of electronic and and nuclear parts. The exchange potential was calculated from the local approximation due to Slater[22]:

$$V_x(\underset{\sim}{r}) = -6\left[\frac{3}{8\pi}\ \rho(\underset{\sim}{r})\right]^{1/3} \qquad (3)$$

Finally, contributions to the potential in the C_2H_2 atomic spheres from substrate interaction was approximated by simple overlap of platinum potentials using standard methods.[15]

We generally have used overlapping atomic spheres on the carbon and hydrogen atoms; this departure from a strict muffin-tin treatment was made in order to include more of the electronic charge, a substantial portion of which lies outside of non-overlapping spheres. This problem has been dealt with earlier in connection with electronic structure calculations with the SCF Xα scattered-wave method[24] and arises, for example, in organic molecules with π-electron systems.

In the Appendix, however, we compare I-V profiles calculated using phase shifts derived from both overlapping and non-overlapping sphere

parameterizations, and we demonstrate that differences are too small to influence structural determinations.

In Table II we list the muffin-tin potential for carbon in C_2H_2 obtained by the above method and compare this potential to that of atomic carbon.[25] We note that these two potentials are nearly identical for small radii (as expected) and that their difference at the sphere radius (r_C = 1.50 au) is only 0.2 Rydberg. This similarity is obtained, of course, only because we have spherically averaged around each of the acetylenic carbon atoms. If one compares, for example, the electrostatic potential $\Phi(\underset{\sim}{r})$ along the C-C bond direction with the potential at the same radius perpendicular to the C-C bond, differences up to ~1 Rydberg are found corresponding to the buildup of bonding charge between the carbon atoms. Given the similarity of the spherically-averaged acetylenic-carbon potentials to those derived from the corresponding atom we have accordingly employed atomic hydrogen potentials to approximate the hydrogen scattering in acetylene, as indicated in Table II.

Phase shifts (δ_ℓ) derived from the muffin-tin potentials of carbon and hydrogen are shown in Figs. 2-3. Their behavior with energy is very similar to but they differ quantitatively from the corresponding free atom phase shifts[26] since the potentials are truncated at the sphere radii r_C and r_H given in Table II. We note that the s, p and d-waves are quite strong for carbon whereas the hydrogen scattering is weak with only the s-wave being relatively strong. We may also compare relative elastic scattering cross sections determined from the phase shifts. At 80 eV,

for example, the platinum cross section is over 3 times larger than the carbon cross section and 25 times larger than the hydrogen cross section.

Room-temperature vibrations of carbon and hydrogen were included in the analysis using the conventional Debye-Waller factor approach and assuming spherically-symmetric vibrational amplitudes. The vibrational amplitude of the molecule was estimated from experimental measurements on metal-alkyne clusters which generally show a frequency of 400-600 cm^{-1} for metal-acetylene stretching modes. The actual amplitude of vibration at room-temperature is relatively small, comparable to that of platinum, and hence the Debye-Waller corrections are of minor significance in the energy range below 100 eV.[19]

Intensity Averaging Over Equivalent Domains

The observed diffraction pattern for the acetylene overlayers may arise from domains of either (2x2) or (2x1) real space unit cells. In the case of (2x1) periodicity the presence of the three equivalent 120°-rotated domains of the molecule on the surface would be essential to produce the necessary spots that give a nominal (2x2) diffraction pattern. In the case of either (2x1) or (2x2) symmetry, however, the presence of equal numbers of the three domains is also necessary since unequal mixtures would not give the observed threefold symmetry of the spot intensities.

The small size, high intensity and good definition of the fractional-order diffraction spots indicates that order in the overlayer persists on a scale comparable to or larger than the coherence width of the electron beam (~100 Å). We make the assumption that only one of the three rotational orientations is present within a given coherence zone, i.e., we assume that boundary effects may be neglected. This assumption is valid providing either that the domains of a given orientation are much larger than the coherence zone or that no particular phase relation connects different domains. With this assumption it is only necessary to average together intensities (as opposed to adding amplitudes) calculated for the three orientations. For a general incident beam angle (θ,ϕ) this procedure then involves three independent intensity calculations. However, along high-symmetry azimuths (ϕ) only two calculations are necessary, and at normal incidence $(\theta=0°)$ only one calculation is needed.

It has been noted that a (2x1) overlayer is unlikely in the light of both helium scattering results as well as consideration of van der Waals radii.[27] However, in the absence of quantitative coverage data we carried out calculations for (2x1) overlayer geometries at normal incidence. We did not find acceptable agreement for the (2x1) acetylene lattice with the observed I-V profiles and in the following section, then, we consider only results for (2x2) arrangements.

IV. RESULTS

In this section we present and discuss the I-V profiles calculated for the various model geometries shown schematically in Fig. 1 as representing, we believe, the likely chemisorption arrangements of acetylene on the Pt(111) surface. Acceptable structures for both the metastable and stable acetylene states were found within the manifold of trial geometries as discussed below. The CC bond length and CCH angle were also studied as described in the Appendix but sensitivity was unfortunately too limited to permit a reliable determination of these parameters. Calculated I-V profiles reported in this section are accordingly restricted to a CC length of 1.20 Å and electron scattering by hydrogen is neglected. However, we suggest (see Appendix) that analysis of high-order beams under conditions of glancing electron incidence may markedly enhance sensitivity to in-plane bond lengths such as the CC length in adsorbed C_2H_2.

The experimental data base for the intensity analysis was obtained by Stair and Somorjai[1] using a rapid photographic collection method with automated scanning.[28] Intensity-voltage profiles were measured for fractional and integral-order beams at incident polar angles in the range $\theta = 0°$-16° along a high-symmetry azimuth, $\phi = 0°$. The measurements generally extended over the energy range 10 eV - 200 eV but little sensitivity to the C_2H_2 adsorbate is found above ~100 eV.[1] All of the experimental I-V profiles for both the metastable and stable C_2H_2 structures were checked for reproducibility after ion-sputtering and oxygen cleaning of the Pt(111) crystal, and data from the stable C_2H_2 structure was checked at $\theta = 0°$ after repolishing the crystal. Good reproducibility of major and minor features in the I-V profiles was demonstrated.[1]

The I-V profiles were calculated for several fractional and integral-order beams at incident angles of θ= 0°, 4°, 8° and 16° in the energy range 15 - 95 eV as outlined in Sec. III. In the analysis below we focus attention on the fractional-order beams since they are most sensitive to the overlayer-substrate registry. The planar (x, y) position of the molecule (Fig. 1) was varied to include high-symmetry sites with the C-C axis parallel to the surface. The z-distance of the molecule above the topmost plane of platinum atoms was varied between 1.3 Å and 2.5 Å. The upper layer z-spacing of the platinum substrate was held fixed at the bulk value determined previously from clean surface studies.[19-20] Thus we assume that the surface platinum atom positions remain invariant during the chemisorption of C_2H_2. The lack of platinum relaxation during adsorption is supported by the experimental observation that the higher energy ($E \gtrsim 100$ eV) I-V peak positions of the integral-order beams, which are dominated by platinum scattering, do not change with acetylene adsorption.[1]

Analysis of the Metastable Acetylene Structure

The optimum agreement between theory and experiment for the metastable C_2H_2 structure is achieved for the atop site coordination (Fig. 1(a)). Comparison of calculated profiles at normal beam incidence for the trial geometries is shown in Figs. 4-5. The results are shown for a z-distance of 2.5 Å which was found to be optimum within 0.1 Å. In Fig. 4 we note that a good fit is indicated for the atop site whereas only marginal agreement between theory and experiment results for the bridging, triangular or di-σ geometries. In Fig. 5 for the $(\frac{1}{2}\,\frac{\tilde{1}}{2})$ beam the fit for the atop site is suggestive but not really adequate since the experimental peak near 55 eV is not reproduced. However, by a small in-plane translation (Δ= 0.25-0.50 Å) from the

atop position (see Fig.15) the agreement is considerably improved.

Similar comparisons for $\theta = 4°$ are shown in Figs. 6-8. The fit for the atop site is quite favorable for all the beams and in every case is superior to the other trial geometries. However, a small displacement Δ from the atop site again appears to improve the agreement as indicated in the range 60-100 eV for the beams shown in Figs. 7-8.

In Fig. 9 a comparison is shown at $\theta = 8°$ for the $(\frac{1}{2}\ 0)$ beam. For this beam the features in the energy range 20-50 eV are seen to be very sensitive to the displacement Δ, and the shifted atop position is again favored. (The agreement in all cases worsens when Δ exceeds ~0.50 Å.)

We conclude on the basis of these and other comparisons that the C_2H_2 molecule in the metastable adsorption state is situated near the atop site at a z-distance of 2.45±0.10 Å; it is very probably slightly displaced from the direct on-top position by ~0.25 Å (cf. Fig. 15).

Analysis of the Stable Acetylene Structure

The best fit to the intensity data for the stable C_2H_2 structure is found for the triangular site coordination (Fig. 1(d)). In Fig. 10 comparison of calculated and experimental I-V profiles at normal incidence is shown for the z-distance of 1.9 Å (the optimum spacing for the stable state). The normal incidence data serves to rule out the atop site geometry but discrimination among the triangular, di-σ, and bridging geometries is not accomplished. However, as shown in Fig. 11 for $\theta = 4°$ and Figs. 12-14 for $\theta = 8°$, the non-normal incidence data clearly favors the triangular geometry over the di-σ and bridging configurations. We note, for example, the very good agreement found for the triangular geometry for the $(\frac{1}{2}\ \frac{\bar{1}}{2})$ and $(\frac{1}{2}\ 0)$ beams at $\theta = 4°$ and the $(\frac{\bar{1}}{2}\ \frac{\bar{1}}{2})$ and $(\frac{1}{2}\ 0)$ beams at $\theta = 8°$; the corresponding

fits for the di-σ and bridging structures are generally poor.

The sites identified in the present analysis for both the metastable (M) and stable (S) adsorption states of C_2H_2 on Pt(111) are illustrated in Fig. 15. We note that there are two inequivalent triangular sites within the surface unit cell corresponding to the presence or absence (hole site) of a Pt atom in the second layer. As indicated in Fig. 15, the triangular site preferred in the stable state in over the hole site. In addition, we also found that the optimum site for the metastable state is slightly displaced from the atop site in the direction of the triangular position which has a Pt atom directly below in the second layer. Relevant C-Pt bond lengths for each structure are given in Fig. 15.

CONCLUSIONS

In conclusion, we have employed dynamical LEED theory to identify two different chemisorption states of acetylene on the Pt(111) surface. In the metastable state the C_2H_2 is basically coordinated to one surface Pt atom. In view of the rather large Pt-C distance of 2.5 Å involved for this state it seems probable that the molecule is weakly perturbed from its gas phase configuration. We suggest that the principal component of the bond involves overlap of the occupied π_u orbitals of C_2H_2 with hybrid Pt orbitals; the back-bonding component to the π_g orbitals is likely small. Support for this contention is provided by data on mononuclear Pt-acetylene complexes; for the class of complexes having rather large Pt-C distances (as large as 2.28(3) Å) the acetylene ligand is comparatively unperturbed, i.e., the R-group cis-bending is less than 20° and the CC bond stretch is less than 0.04 Å.[29]

The transition from the metastable to stable C_2H_2 state has been shown to entail a very sizeable Pt-C bond length contraction of ~0.3 Å and a coordination change from one to three metal atoms. The strengthening of the Pt-C bonds is presumably accompanied by a weakening of the C-C bond, and the coordination to three metal atoms suggests the formation of symmetric carbon-platinum σ bonds (Fig. 1(d)) as occurs in various trinuclear metal-acetylene complexes.[6]

Finally, some remarks on the LEED analysis itself are appropriate. The agreement between calculated and experimental profiles, although never precise, was very encouraging for the optimum structures and comparable to the best fits achieved in previous analyses of atomic chemisorption. Resolution of the high-symmetry candidate structures is comparatively

straightforward providing data for several diffraction angles is analyzed; extensive statistical analysis does not seem at this stage of refinement to be essential. The insensitivity to hydrogen scattering was anticipated, but the lack of significant sensitivity to the CC length was an unexpected and discouraging aspect of the analysis. We are presently exploring the possibility of enhancing the resolution of the CC length by means of a glancing incidence experiment (see Appendix).

Lastly, we would like to emphasize the important role of the multiple-scattering of the electrons; were it not for the wealth of detail in the low-energy region ($E \lesssim 100$ eV) of the fractional-order beam I-V profiles (which arises from multiple-scattering) the adsorbate-substrate registry could not, in the present example, have been resolved. It is, therefore, a major irony that the very multiple-scattering effects which complicate the LEED analysis (and which have often been either neglected or "averaged out") indeed provide the crucial diffraction information necessary to elucidate the adsorbate-substrate registry.

ACKNOWLEDGMENTS

It is a pleasure to acknowledge stimulating discussions with P. C. Stair on numerous aspects of this work. This work was carried out under the auspices of the U. S. Energy Research and Development Administration.

APPENDIX

A. Sensitivity Analysis of Carbon-Carbon Bond Length and CCH Angle Variations

Ideally a LEED intensity analysis of chemisorbed molecules is capable of providing quantitative information on intramolecular bond lengths and bond angles. We have found, however, in the present analysis of acetylene chemisorption little sensitivity to either a CC bond stretch of 0.14 Å ($C \equiv C \rightarrow C = C$) or a CCH angle distortion of up to 60°. The CC bond length analysis is illustrated in Fig. A1 for three fractional-order beams at non-normal incidence. The intensity profiles exhibit only very minor changes in relative intensity which are evident only upon close investigation.

Sensitivity to hydrogen scattering is decidedly greater but still minor as shown in Fig. A2. For the $(\frac{1}{2}\ \bar{\frac{1}{2}})$ beam there is a relative increase in the intensity of the major peak at 35 eV to the very low-energy peak developing near 15 eV as the CCH angle bend is increased. This is a very unreliable criterion to use for structural analysis, however, as the intensity of the peak near 15 eV is strongly affected by reflection at the vacuum-surface barrier, a factor not included in these calculations. The $(\frac{1}{2}\ \frac{1}{2})$ beam (which was not experimentally determined at $\theta = 4°$) does exhibit an interesting intensity-ratio change in the doublet peak occurring near 60 eV. A systematic analysis of such changes in this energy region could lead to a reliable CCH angle determination provided a large number of beams and incident angles were carefully analyzed. However, this would at the same time require a careful sensitivity analysis of other structural and non-structural parameters which may influence such peak

ratio modulations.

Some general comments on the reasons for the notable insensitivity to the intramolecular bond length and bond angle changes are appropriate here. The hydrogen scattering (see text) is, of course, very much weaker than either the carbon or platinum scattering and this fact accounts for the general insensitivity to CCH angle variations. Several factors may contribute to insensitivity to the CC bond length variations, but perhaps the major reason is due to the in-plane orientation of the C-C axis; this orientation implies that a variation Δx in the CC length will only be "seen" by the in-plane components of the scattering vectors. In conventional LEED diffraction experiments operating with the incident electron beam at near-normal incidence ($\theta \lesssim 15°$) the diffracted beams which are typically monitored are those having a very small in-plane momentum-transfer $\underset{\sim}{g}$ but with a relatively large transfer Δk_z in the direction normal to the surface. For a first-order fractional-order beam at $\theta \sim 0°$, $E \sim 50$ eV we have $\underset{\sim}{g} \sim 1.3$ $\mathring{A}^{-1}$ whereas $\Delta k_z \sim 7$ $\mathring{A}^{-1}$, implying that a phase change of say $\Delta\phi \sim \frac{\pi}{4}$ is produced by $\Delta z \sim 0.1$ $\mathring{A}$ but requires $\Delta x \sim 0.5$ $\mathring{A}$. Hence, we expect under these diffraction conditions adequate sensistivity to out-of-plane/(Δz) changes but very poor resolution of in-plane (Δx) changes, precisely as has been found in all LEED analyses reported to date.

We may note that by employing a more nearly glancing incidence diffraction geometry ($\theta \gtrsim 60°$), the parallel components of all the allowed diffraction beams are systematically increased over those at $\theta \sim 0°$; beams having $g \sim 7$ $\mathring{A}^{-1}$ would be observable with conventional LEED instrumentation at $\theta = 60°$, for example. Hence, it seems quite probable that improved resolution of in-plane bond lengths and overlayer-substrate

registries can be achieved by analysis of the high-order beams near glancing incidence.

B. Sensitivity Analysis of Non-Structural Parameters

In this section we consider the influence of two sets of non-structural parameters related to the construction of the acetylene scattering potential. We examine (1) sensitivity to a change in the average value of the potential between muffin-tin spheres in the overlayer ("inner potential") relative to the substrate value (V_o = 14.3 eV) and (2) sensitivity to different sets of phase shifts derived from overlapping (r_c = 1.50 au) and non-overlapping (r_c = 1.14 au) sphere parameterizations of the carbon scattering. Both sets of parameters are *a priori* undetermined although an uncertainty in the overlayer inner potential of 5-10 eV is expected and the muffin-tin radii given above would seem to represent reasonable limits.

In Fig. A3 results are shown for three sets of parameter choices for two fractional-order beams. The lower two profiles in each panel compare sensitivity to the muffin-tin radii whereas the topmost and lowest curves compare results for a ΔV_o = -5 eV in the overlayer inner potential. There is somewhat greater sensitivity to the muffin-tin radius change, but each parameter choice introduces relatively minor changes in the lineshapes. Hence, we conclude that reasonable variations in these non-structural parameters do not influence the calculated I-V profiles to a degree significant enough to affect the structural determinations.

Table I. Examples of bonding structures and bond lengths for acetylenic ligands (RC ≡ CR) in various transition-metal complexes.*

Compound	Bonding Geometry	Average M-C (Å)	C ≡ C (Å)	CCR Angle (degrees)
$(Ph_3P)_2Pt(C_2Ph_2)$[a]	one-coordinate π	2.04	1.32	140
$(CO)_6Co_2(C_2Ph_2)$[b]	bridging (μ)	1.97	1.37	138
$(\eta^5\text{-}C_5H_5)_2Rh_2(CO)_2(CF_3C_2CF_3)$[c]	di-σ	2.04	1.29	130
$Os_3(CO)_{10}(C_2Ph_2)$[d]	triangular	2.22	1.29	†

a J. O. Glanville, J. M. Stewart and S. O. Grim, J. Organometal. Chem. 7,P9 (1967).

b W. G. Sly, J. Am. Chem. Soc. 81, 18 (1959); D. A. Brown, J. Chem. Phys. 33, 1037 (1960).

c R. S. Dickson, H. P. Kirsch and D. J. Lloyd, J. Organometal. Chem. 101, C48 (1975).

d M. Tachikawa, J. R. Shapley, C. G. Pierpont, J. Am. Chem. Soc. 97, 7174 (1975).

* For reference, the carbon-carbon single-bond length (parafinnic) is 1.54 Å, the double-bond length (olefinic) 1.34 Å and the triple-bond length (acetylenic) 1.20 Å.

† CCR angle not reported.

Table II. Muffin-tin potentials for carbon and hydrogen†

[-rV(r)(au)]

r	Carbon in C_2H_2	Atomic Carbon	Atomic Hydrogen
0.00	12.00	12.00	2.00
0.25	8.46	8.45	1.94
0.50	6.26	6.27	1.82
0.75	5.06	5.05	1.70
1.00	4.32	4.21	1.58
1.20	3.92	3.67	1.48
1.50	3.36	3.05	1.36

† C-C distance = 2.28 au

C-H distance = 2.00 au

r_C = 1.50 au (muffin-tin radius)

r_H = 0.86 au (muffin-tin radius)

REFERENCES

1. P. C. Stair and G. A. Somorjai, Chem. Phys. Lett. 41, 391 (1976); J. Chem. Phys. (in press).

2. J. E. Demuth, Chem. Phys. Lett. 45, 12 (1977).

3. W. J. Lo, Y. W. Chung, L. L. Kesmodel, P. C. Stair and G. A. Somorjai, Solid State Commun. (to be published)..

4. L. L. Kesmodel, P. C. Stair, R. C. Baetzold and G. A. Somorjai, Phys. Rev. Lett. 36, 1316 (1976).

5. See, e.g., L. L. Kesmodel and G. A. Somorjai, Accts. Chem. Res. 9, 392 (1976) and references therein.

6. See, e.g., R. Mason and K. M. Thomas, Ann. N. Y. Acad. Sci. 238, 225 (1974) and references therein.

7. A "μ" bond is defined as the interaction by direct overlap of a σ orbital of a metal atom with an electron-donating π orbital of an unsaturated hydrocarbon (P. L. Pauson, Proc. Chem. Soc. 297 (1960)). It is commonly used to describe the metal-acetylene bonds in organometallic clusters with "bridging" acetylenes.

8. G. C. Bond, Catalysis by Metals (Academic, New York, 1962); in Advances in Catalysis (Academic, New York, 1964), Vol. 15, p. 91.

9. A. B. Anderson, J. Chem. Phys. 65, 1729 (1976).

10. See Ref. 6 for an extensive presentation of the structures of metal-alkyne complexes.

11. M. J. S. Dewar, Bull. Soc. Chim. Fr. 18, C79 (1951); J. Chatt and L. A. Duncanson, J. Chem. Soc. 2939 (1953).

12. For an elementary discussion of bonding in mononuclear and binuclear metal-alkyne complexes see, e.g., R. B. King, Transition-Metal

Organometallic Chemistry (Academic, New York, 1969).

13. J. E. Demuth and D. E. Eastman, Phys. Rev. Lett. 32, 1123 (1974); Phys. Rev. B 13, 1523 (1976).

14. See, e.g., J. B. Pendry, Low-Energy Electron Diffraction (Academic, London, 1974).

15. T. Loucks, Augmented Plane Wave Method (Benjamin, New York, 1967).

16. E. Merzbacher, Quantum Mechanics (Wiley, New York, 1967).

17. Ref. 14, p. 141.

18. See, e.g., M. A. Van Hove, Surf. Sci. 48, 406 (1975).

19. L. L. Kesmodel and G. A. Somorjai, Phys. Rev. B 11, 630 (1975).

20. L. L. Kesmodel, P. C. Stair and G. A. Somorjai, Surf. Sci. (in press).

21. O. K. Andersen and A. R. Mackintosh, Solid State Commun. 6, 285 (1968); O. K. Andersen, Phys. Rev. B 2, 883 (1970).

22. J. C. Slater, Phys. Rev. 81, 385 (1951).

23. W. E. Palke and W. N. Lipscomb, J. Am. Chem. Soc. 88, 2384 (1966).

24. N. Rösch, W. G. Klemperer and K. H. Johnson, Chem. Phys. Lett. 23 149 (1973).

25. Atomic wavefunctions taken from E. Clementi, IBM J. Res. and Develop. Suppl. 9, 2 (1965).

26. M. R. Martin (personal communication).

27. D. L. Smith and R. P. Merrill, J. Chem. Phys. 52, 5861 (1970); W. H. Weinberg, H. A. Deans and R. P. Merrill, Surf. Sci. 41, 312 (1974).

28. P. C. Stair, T. J. Kaminska, L. L. Kesmodel and G. A. Somorjai, Phys. Rev. B 11, 623 (1975). A rapid method of data collection is essential in these studies since electron beam damage to the adsorbate occurs on a time-scale of 100 s for typical beam currents.

29. See, e.g., B. W. Davies and N. C. Payne, Can. J. Chem. 51, 3477 (1973) and references therein.

FIGURE CAPTIONS

Fig. 1 Schematic showing various high-symmetry bonding sites for C_2H_2 on the (111) face of an f.c.c. crystal. In each case a simplified picture of the C_2H_2-metal bonding is indicated which corresponds to analogous structures found in organometallic complexes of acetylenes (see text).

Fig. 2 Phase shifts in radians for carbon based on the muffin-tin potential appropriate for acetylene used in this work. A carbon muffin-tin radius (r_C= 1.50 au) was used. Energies are referred to the muffin-tin zero.

Fig. 3 Phase shifts in radians for hydrogen based on an atomic hydrogen potential with the muffin-tin radius (r_H= 0.86 au) used in this work. Energies are referred to the muffin-tin zero.

Fig. 4 Comparison of calculated I-V profiles for the model geometries (Fig. 1) to experiment (Ref. 1) for the metastable C_2H_2 structure for the $(0\ \bar{\frac{1}{2}})$ beam at θ= 0°. The z-distance of the molecule above the topmost plane of the Pt atoms is 2.5 Å, T= 300 K.

Fig. 5 Comparison of calculated and experimental I-V profiles for the metastable C_2H_2 structure for the $(\frac{1}{2}\ \bar{\frac{1}{2}})$ beam at θ= 0°. The effect of a small displacement Δ= 0.5 Å. from the atop position is shown (see Fig. 15). Other conditions as given in Fig. 4.

Fig. 6 Comparison of calculated and experimental I-V profiles for the metastable C_2H_2 structure for the $(0\ \bar{\frac{1}{2}})$ beam at θ= 4°; Δ= 0.25 Å (see Fig. 5, 15). Other conditions as given in Fig. 4.

Fig. 7 Comparison of calculated and experimental I-V profiles for the metastable C_2H_2 structure for the $(\frac{1}{2}\ 0)$ beam at θ= 4°; Δ= 0.25 Å

(see Figs. 5, 15). Other conditions as given in Fig. 4.

Fig. 8 Comparison of calculated and experimental I-V profiles for the metastable C_2H_2 structure for the $(\frac{1}{2}\ \bar{\frac{1}{2}})$ beam at θ= 4°; Δ= 0.25 Å (see Figs. 5, 15). Other conditions as given in Fig. 4.

Fig. 9 Comparison of calculated and experimental I-V profiles for the metastable C_2H_2 structure for the $(\frac{1}{2}\ 0)$ beam at θ= 8°; Δ= 0.50 Å (See Figs. 5, 15). Other conditions as given in Fig. 4.

Fig. 10 Comparison of calculated I-V profiles for the model geometries (Fig. 1) to experiment (Ref. 1) for the stable C_2H_2 structure for the $(\frac{1}{2}\ \bar{\frac{1}{2}})$ and $(0\ \bar{\frac{1}{2}})$ beams at θ= 0°. The z-distance of the molecule above the topmost plane of Pt atoms is 1.9 Å, T= 300 K.

Fig. 11 Comparison of calculated and experimental I-V profiles for the stable C_2H_2 structure for the $(\frac{1}{2}\ \bar{\frac{1}{2}})$and $(\frac{1}{2}\ 0)$ beams at θ= 4°. Other conditions as given in Fig. 10.

Fig. 12 Comparison of calculated and experimental I-V profiles for the stable C_2H_2 structure for the $(\bar{\frac{1}{2}}\ \bar{\frac{1}{2}})$ and $(\frac{1}{2}\ 0)$ beams at θ= 8°. Other conditions as given in Fig. 10.

Fig. 13 Comparison of calculated and experimental I-V profiles for the stable C_2H_2 structure for the $(0\ \bar{\frac{1}{2}})$ and $(\frac{1}{2}\ \bar{\frac{1}{2}})$ beams at θ= 8°. Other conditions as given in Fig. 10.

Fig. 14 Comparison of calculated and experimental I-V profiles for the stable C_2H_2 structure for the $(0\ \bar{1})$ and $(\bar{1}\ 0)$ beams at θ= 8°. Other conditions as given in Fig. 10.

Fig. 15 Schematic of the Pt(111) surface unit cell and the bonding positions of C_2H_2 in the metastable (M) and stable (S) chemisorption states indicated by the LEED analysis (hydrogen atoms are not shown).

Platinum atoms in the first surface layer are represented by open circles and the platinum atom in the second layer is shaded. In the metastable state the molecule is coordinated to essentially one platinum atom but slightly displaced from the atop position as shown, Pt1-C= 2.5(1) Å. In the stable state the molecule is coordinated to three platinum atoms, Pt2-C= 2.2(1) Å, Pt4-C= 2.6(1) Å, etc. Reflection across the dashed verticle line is a symmetry operation for the surface, hence the two carbon atoms are in equivalent bonding positions in each structure.

APPENDIX FIGURE CAPTIONS

Fig. A1 Calculated I-V profiles for C_2H_2 on Pt(111) showing the almost negligible effect of an expansion in the CC bond length from the C≡C length of 1.20 Å to the C=C length of 1.34 Å. The results are shown for low-index fractional-order beams at near-normal beam incidence, $\theta = 8°$.

Fig. A2 Calculated I-V profiles for C_2H_2 on Pt(111) showing the generally low sensitivity to hydrogen cis-bending. Note the reversal in relative intensity for the doublet peak at E~ 60 eV for the $(\frac{1}{2}\ \frac{1}{2})$ beam as the hydrogens are bent away from the surface.

Fig. A3 Calculated I-V profiles for C_2H_2 on Pt(111) showing the effect of variation of the carbon muffin-tin radius (r_C) and a change (ΔV_o) in the relative levels of the overlayer and substrate potentials.

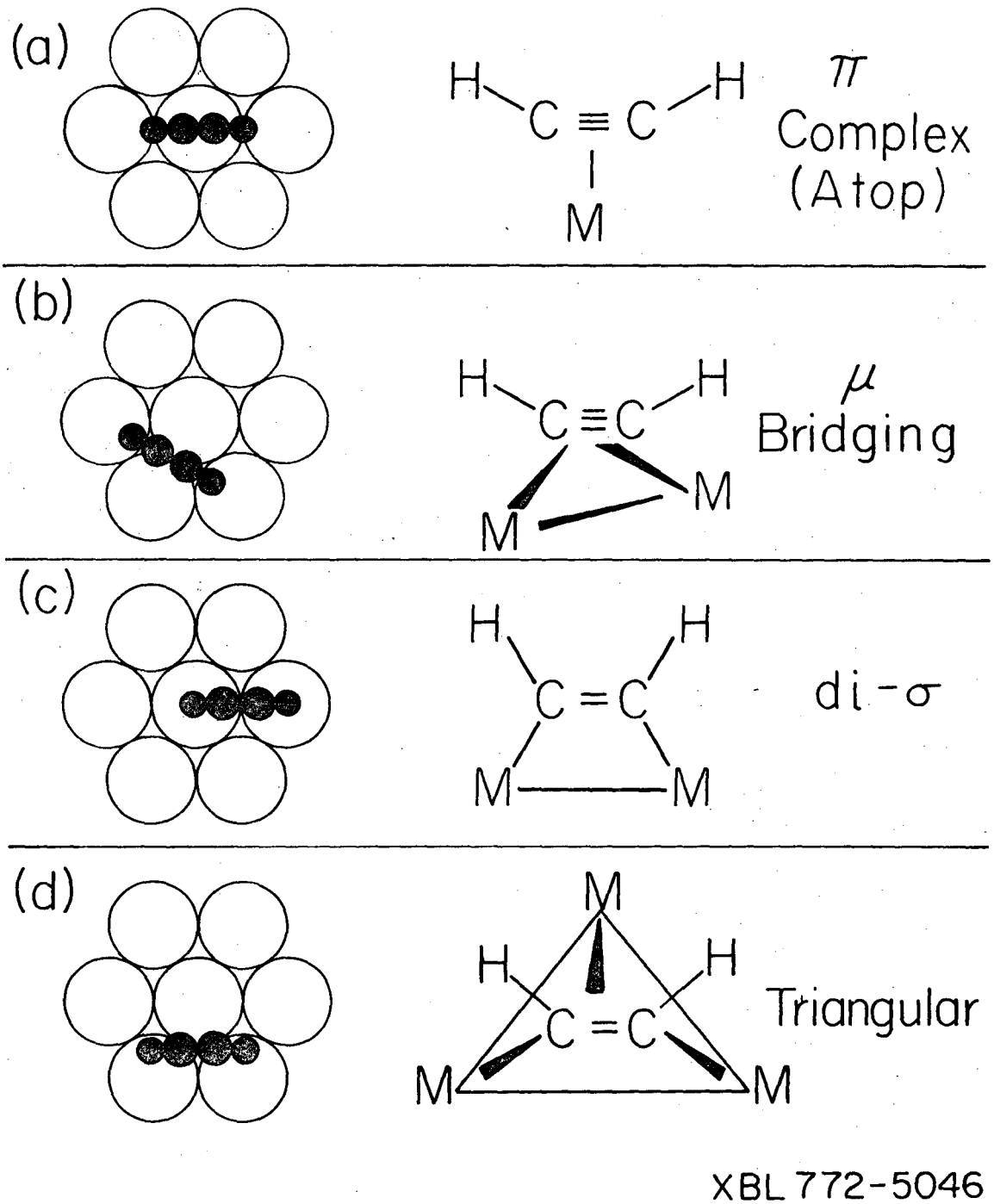
(a)
H
C ≡ C
H
M
π Complex (Atop)
(b)
H
C ≡ C
H
M
M
μ Bridging
(c)
H
H
C = C
M
M
di-σ
(d)
M
H
H
C = C
M
M
Triangular

XBL 772-5046

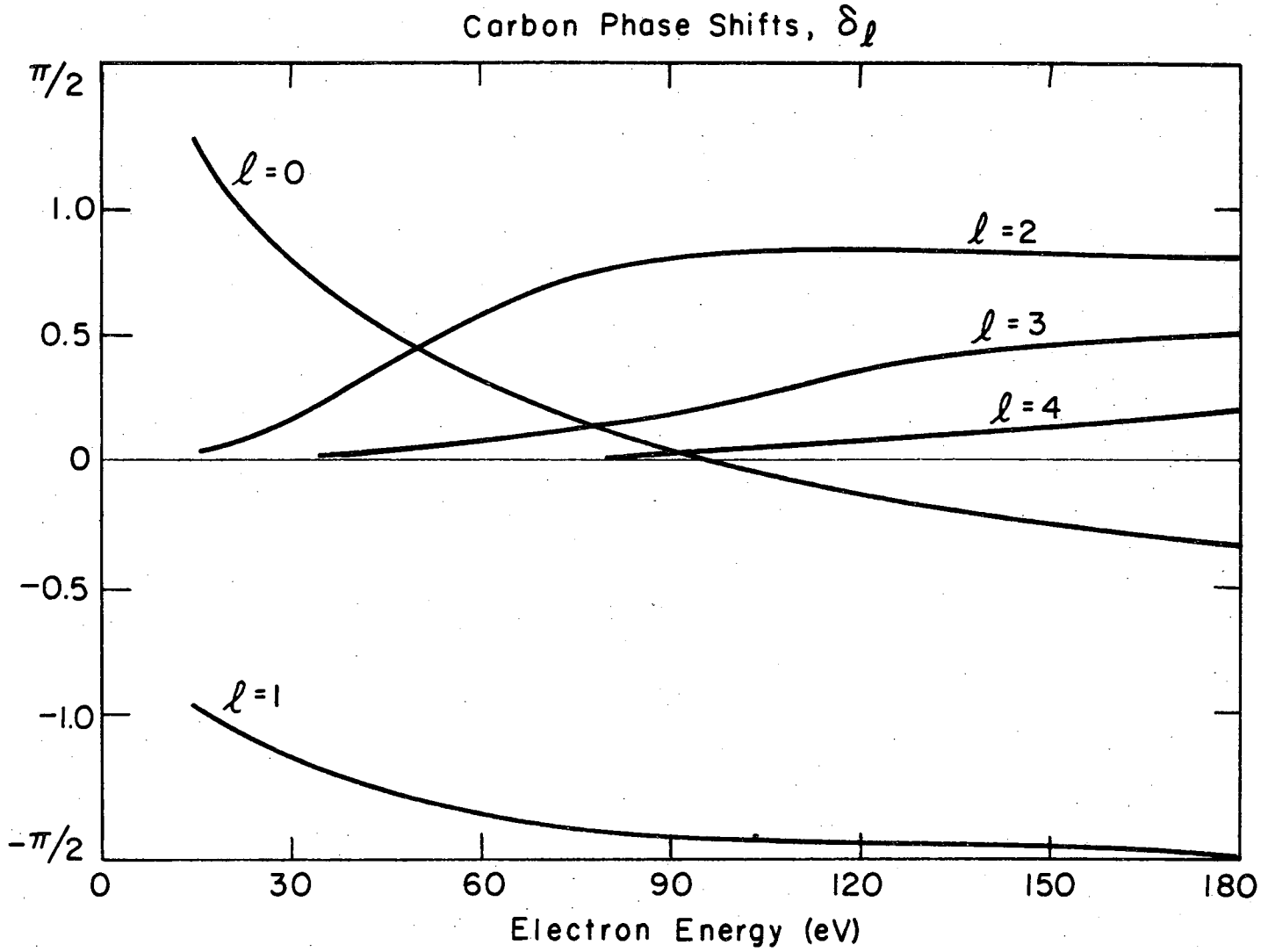

XBL767-7143

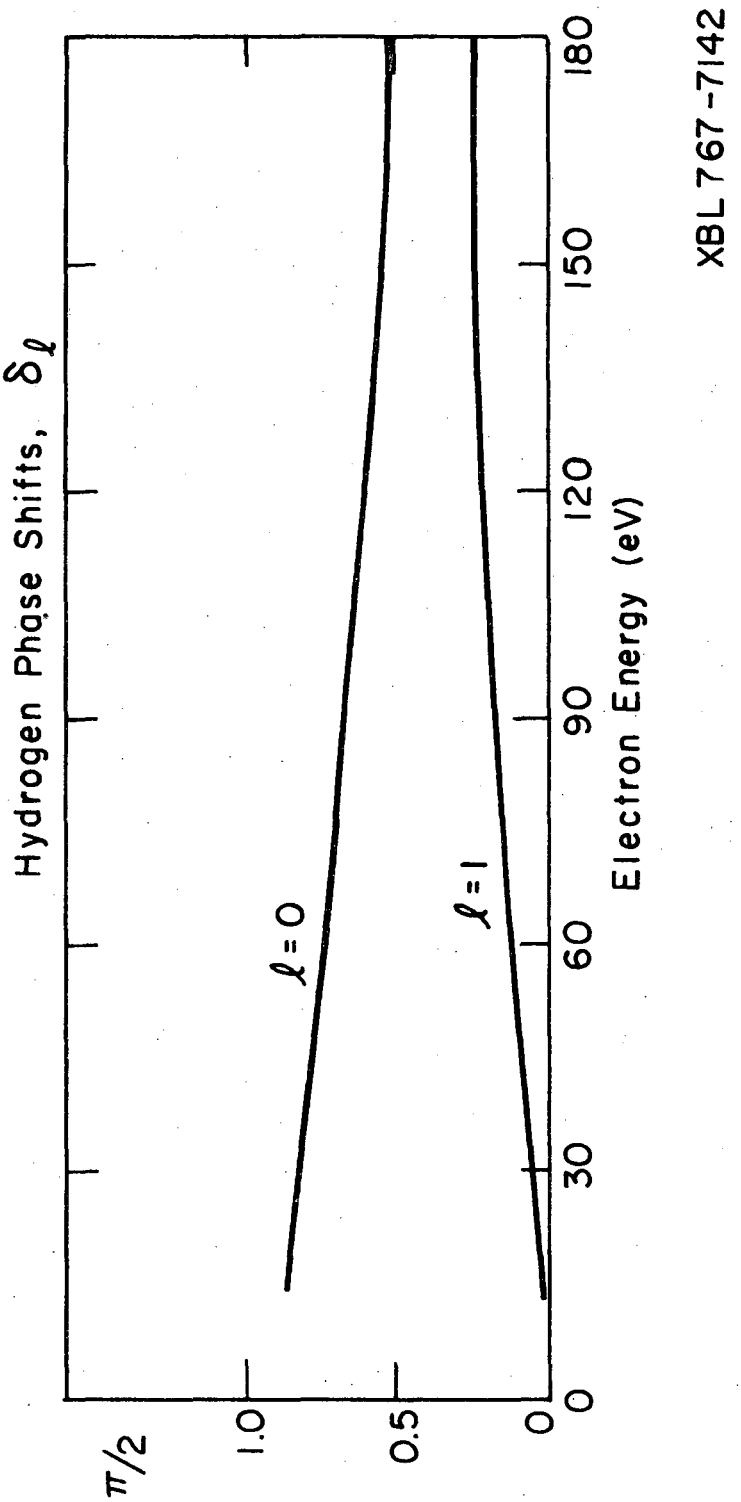

XBL 767-7142

3

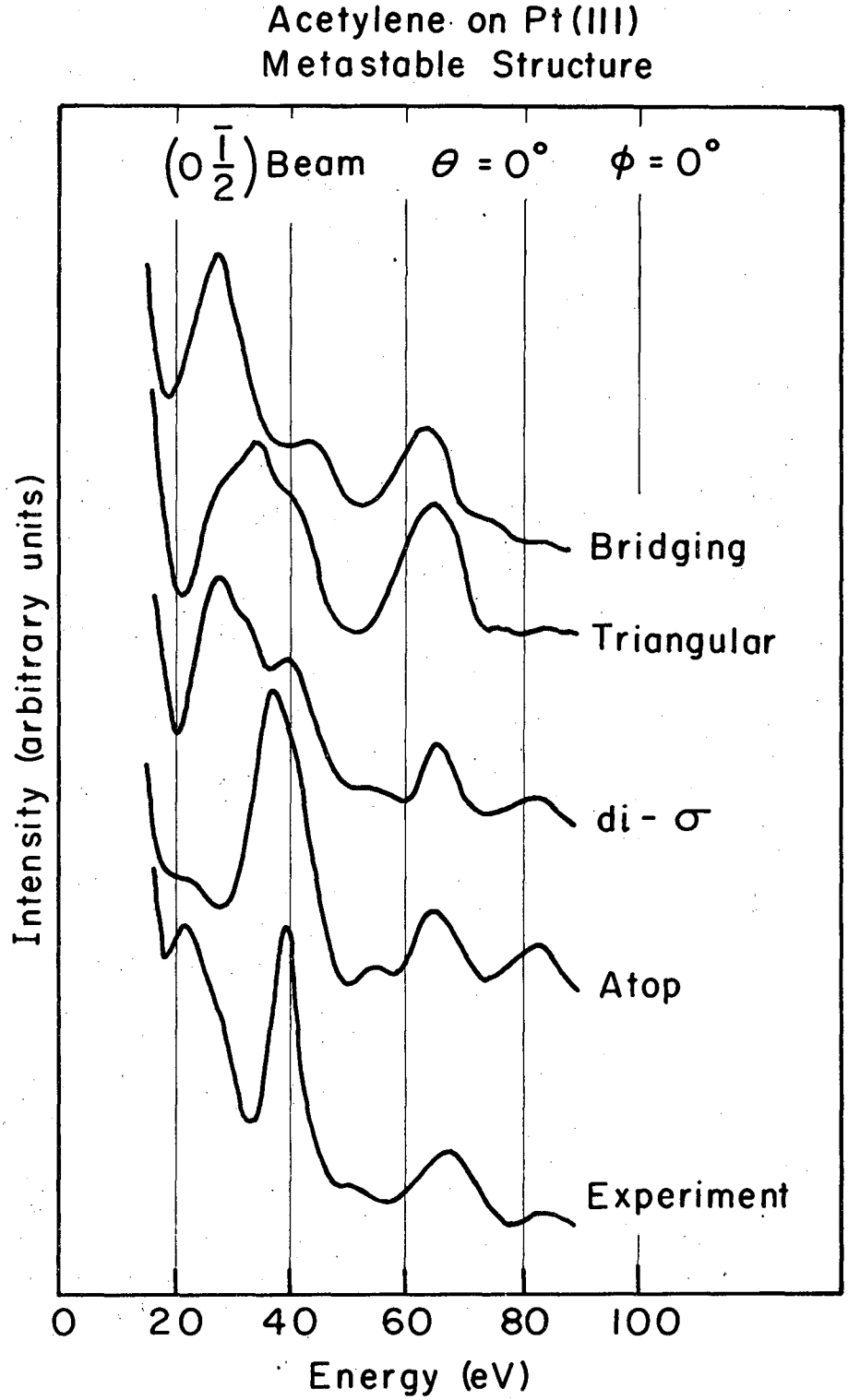

XBL 772-5068

4

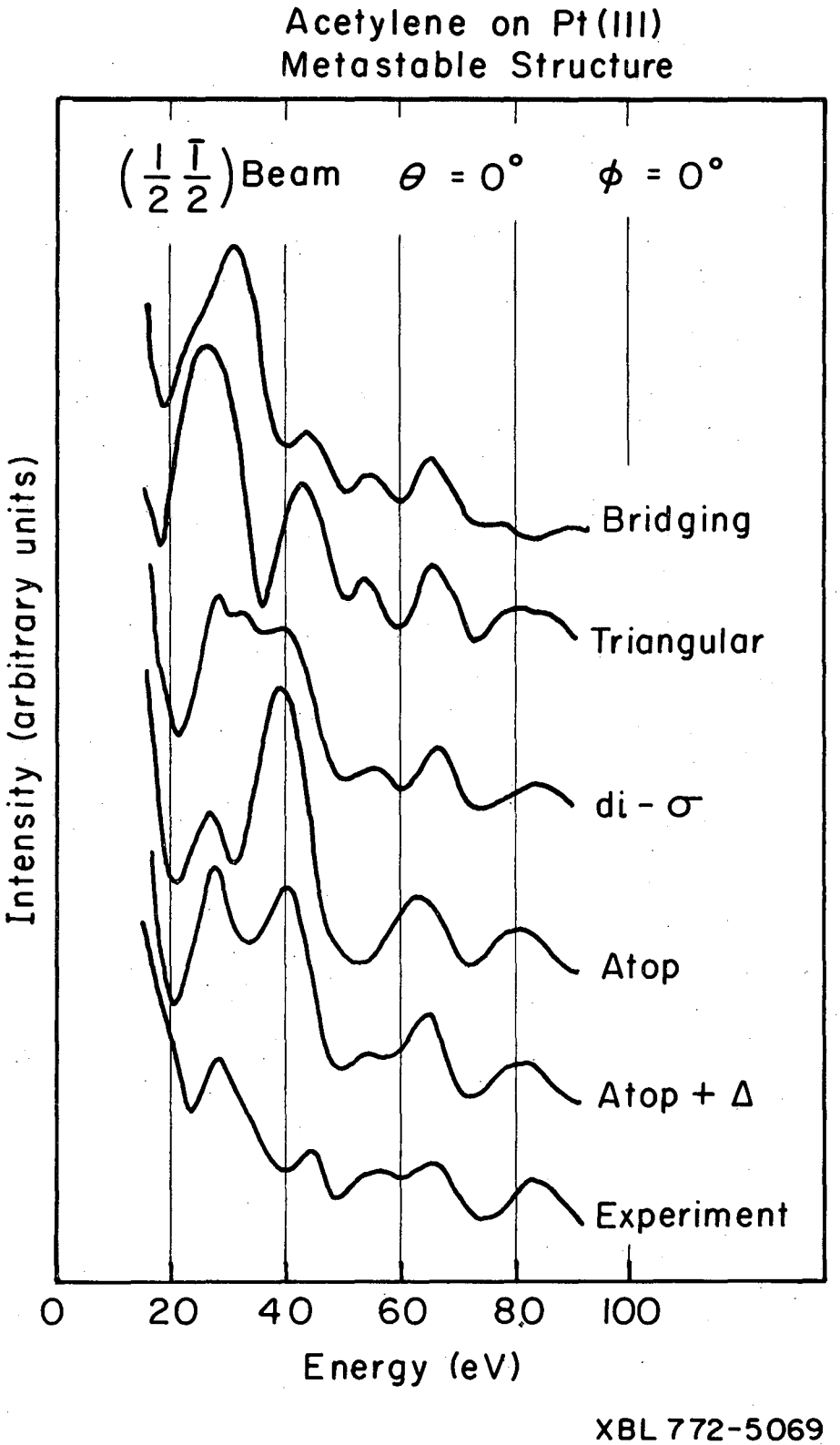

XBL 772-5069

5

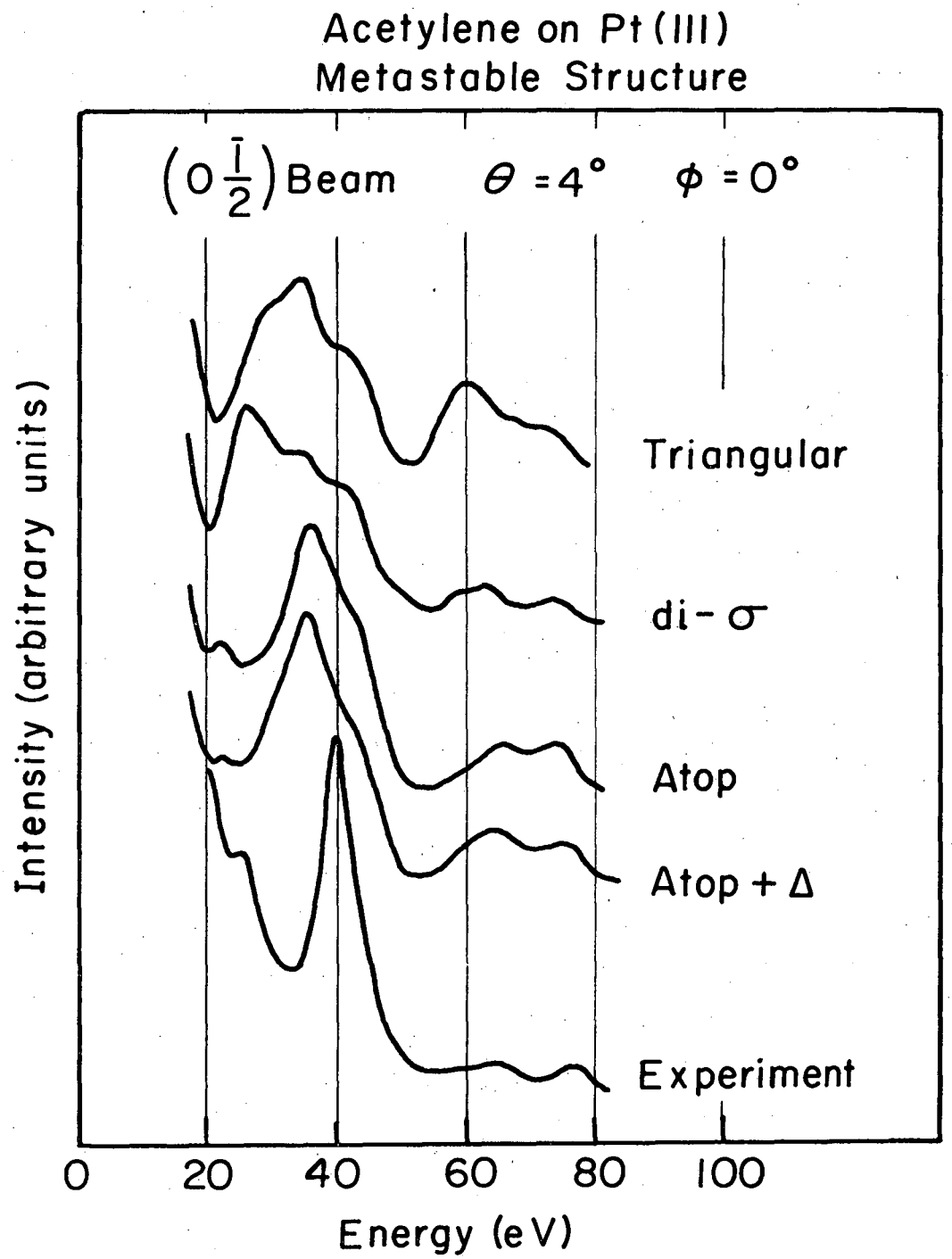
Acetylene on Pt(111)
Metastable Structure
$(0\frac{\bar{1}}{2})$ Beam
$\theta = 4°$
$\phi = 0°$
Triangular
di-σ
Atop
Atop + Δ
Experiment
Intensity (arbitrary units)
0
20
40
60
80
100
Energy (eV)

XBL772-5065

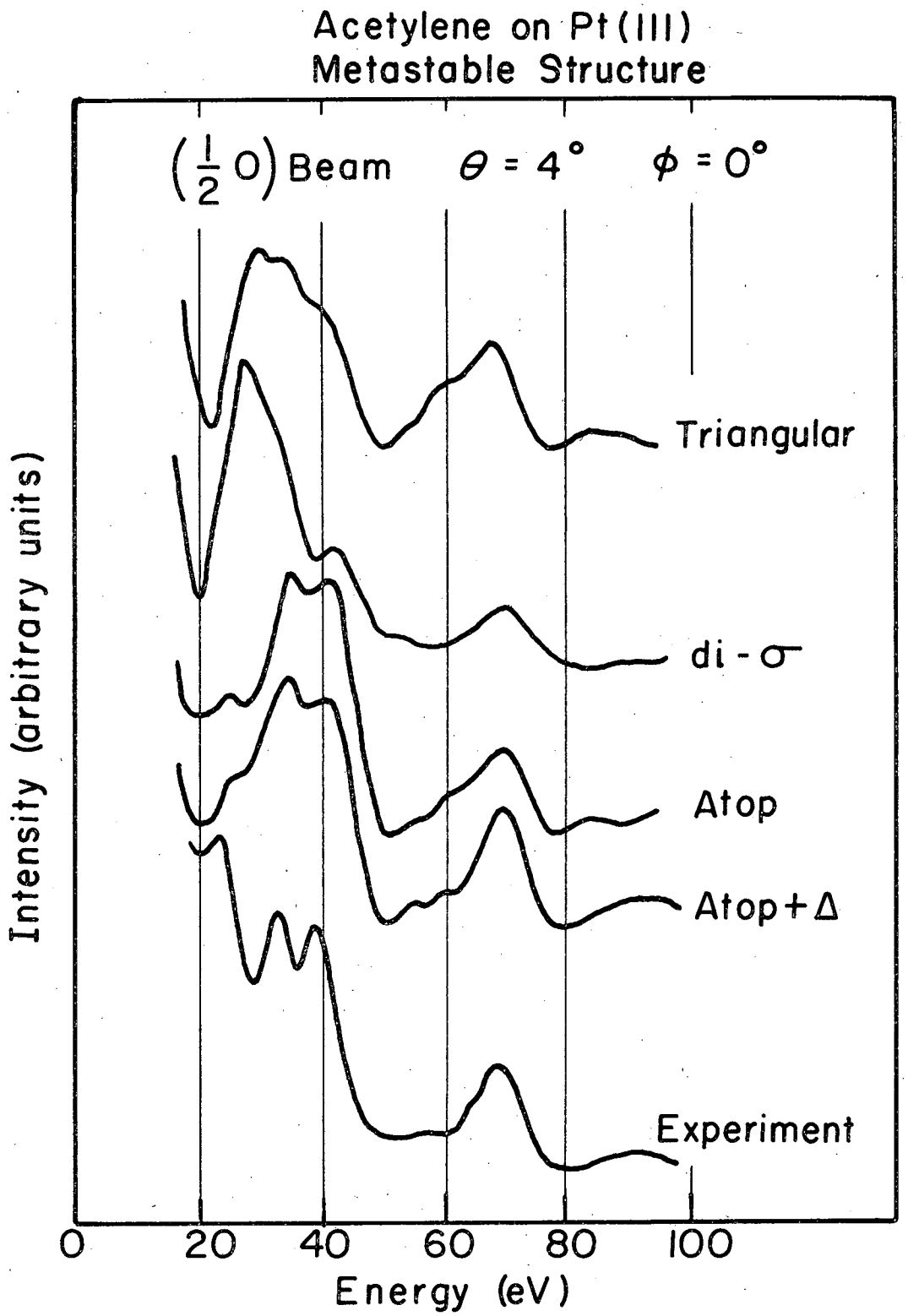
Acetylene on Pt(111)
Metastable Structure
(1/2 0) Beam θ = 4° φ = 0°
Triangular
di-σ
Atop
Atop+Δ
Experiment
Intensity (arbitrary units)
0
20
40
60
80
100
Energy (eV)

XBL 772-5066

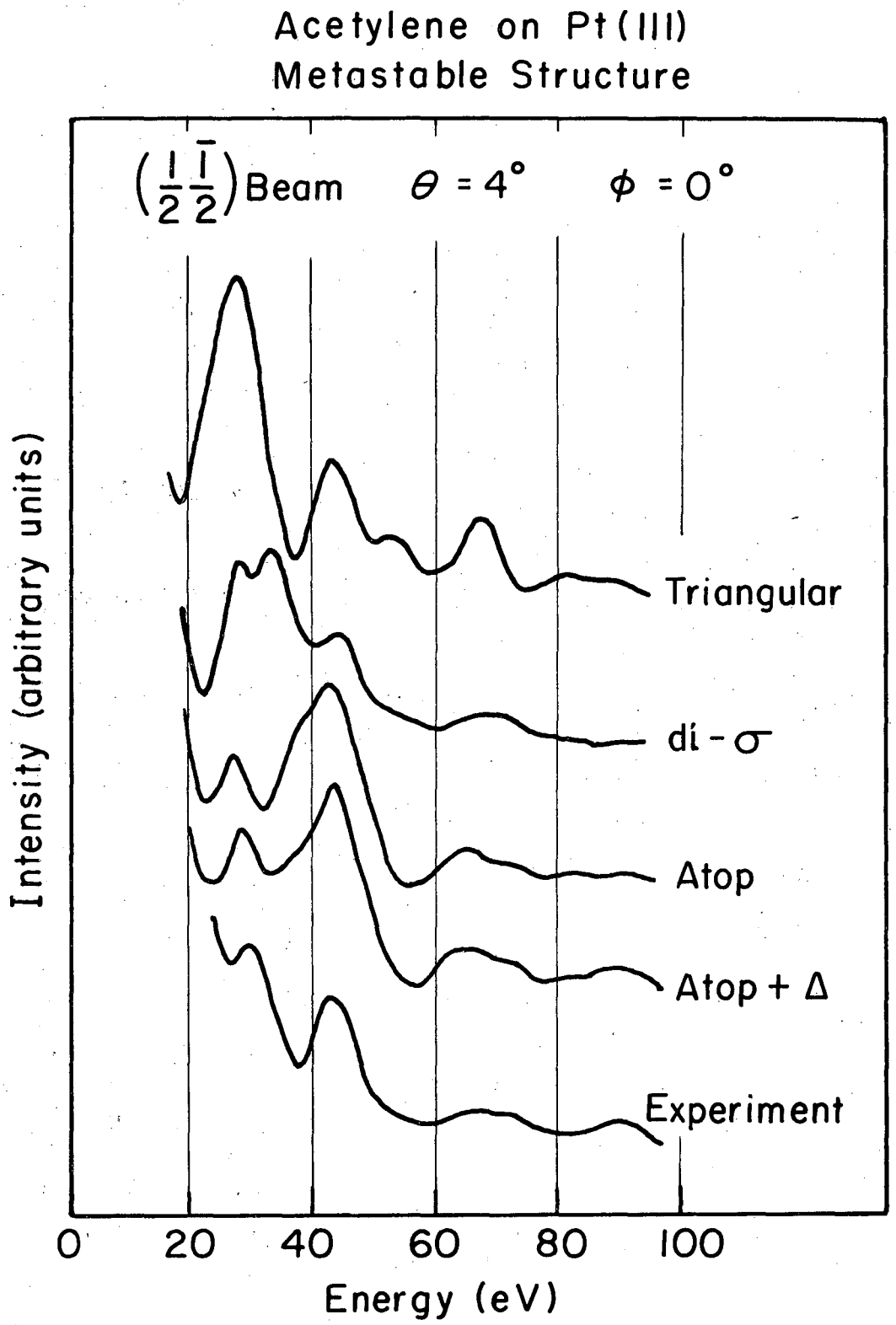

XBL 772-5067

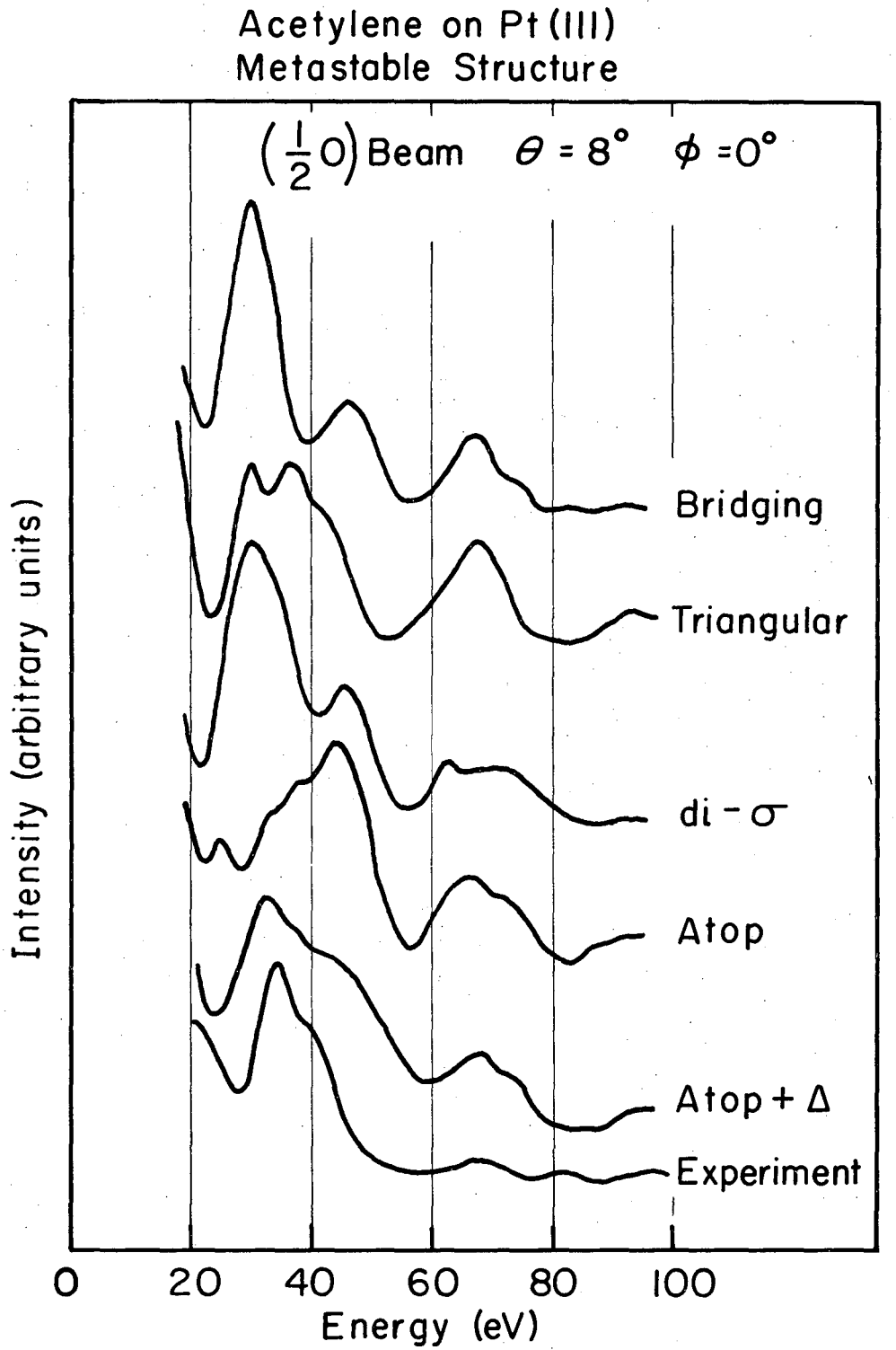
Acetylene on Pt(111)
Metastable Structure
$(\frac{1}{2}0)$ Beam $\theta = 8°$ $\phi = 0°$
Bridging
Triangular
di-σ
Atop
Atop + Δ
Experiment
Intensity (arbitrary units)
0
20
40
60
80
100
Energy (eV)

XBL772-5064

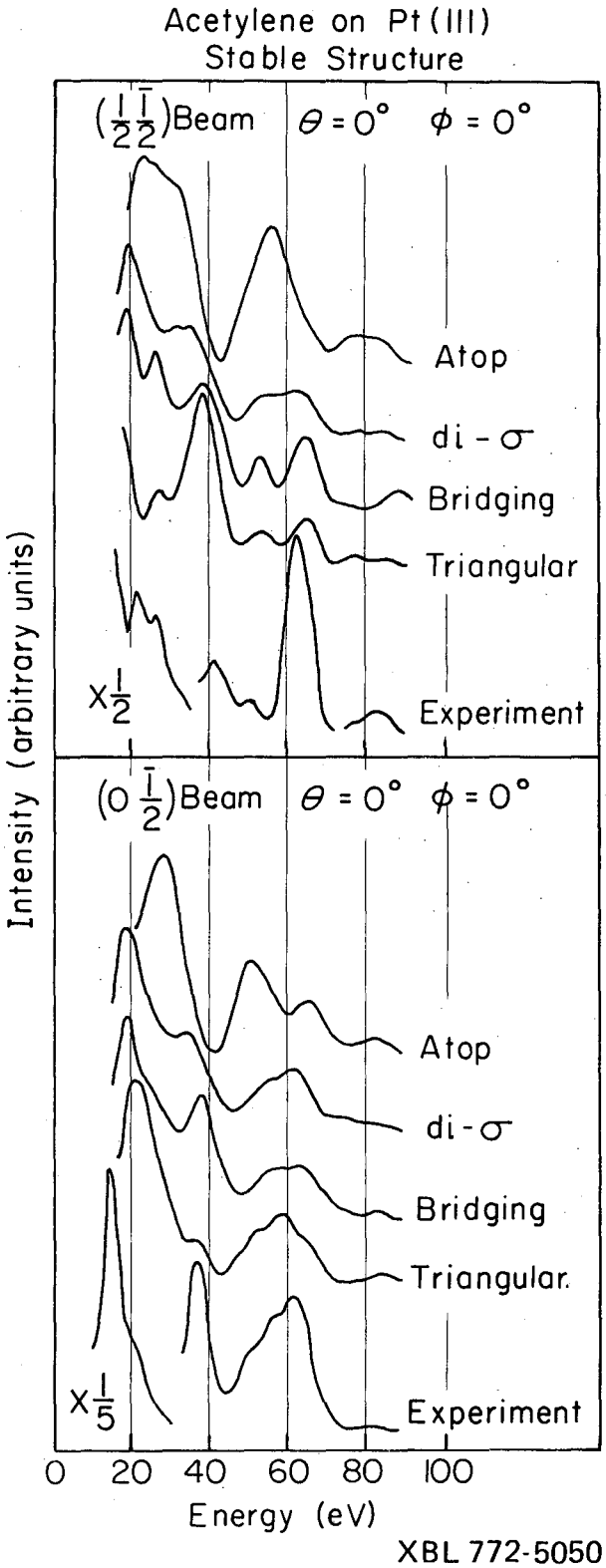
Acetylene on Pt(111)
Stable Structure
$(\frac{1}{2}\frac{\bar{1}}{2})$Beam $\theta = 0°$ $\phi = 0°$
Atop
di-σ
Bridging
Triangular
$\times\frac{1}{2}$
Experiment
$(0\frac{\bar{1}}{2})$Beam $\theta = 0°$ $\phi = 0°$
Atop
di-σ
Bridging
Triangular.
$\times\frac{1}{5}$
Experiment
Intensity (arbitrary units)
0 20 40 60 80 100
Energy (eV)

XBL 772-5050

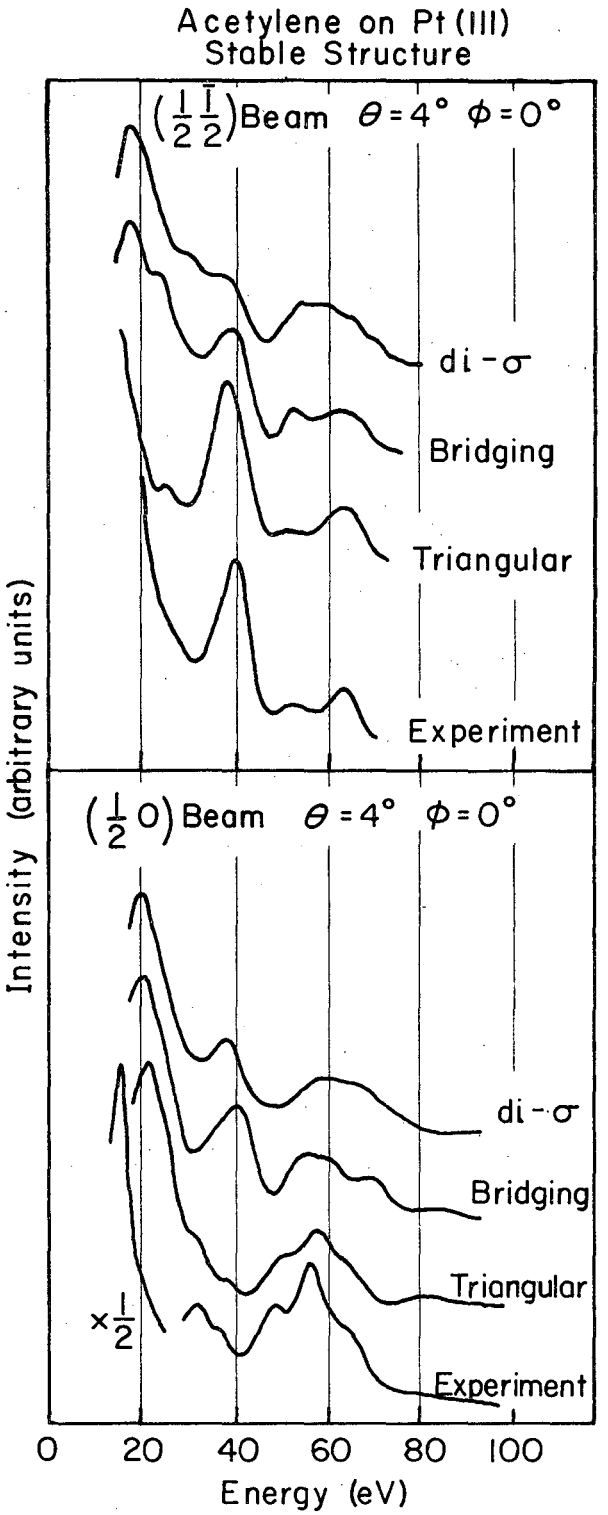

XBL772-5051

11

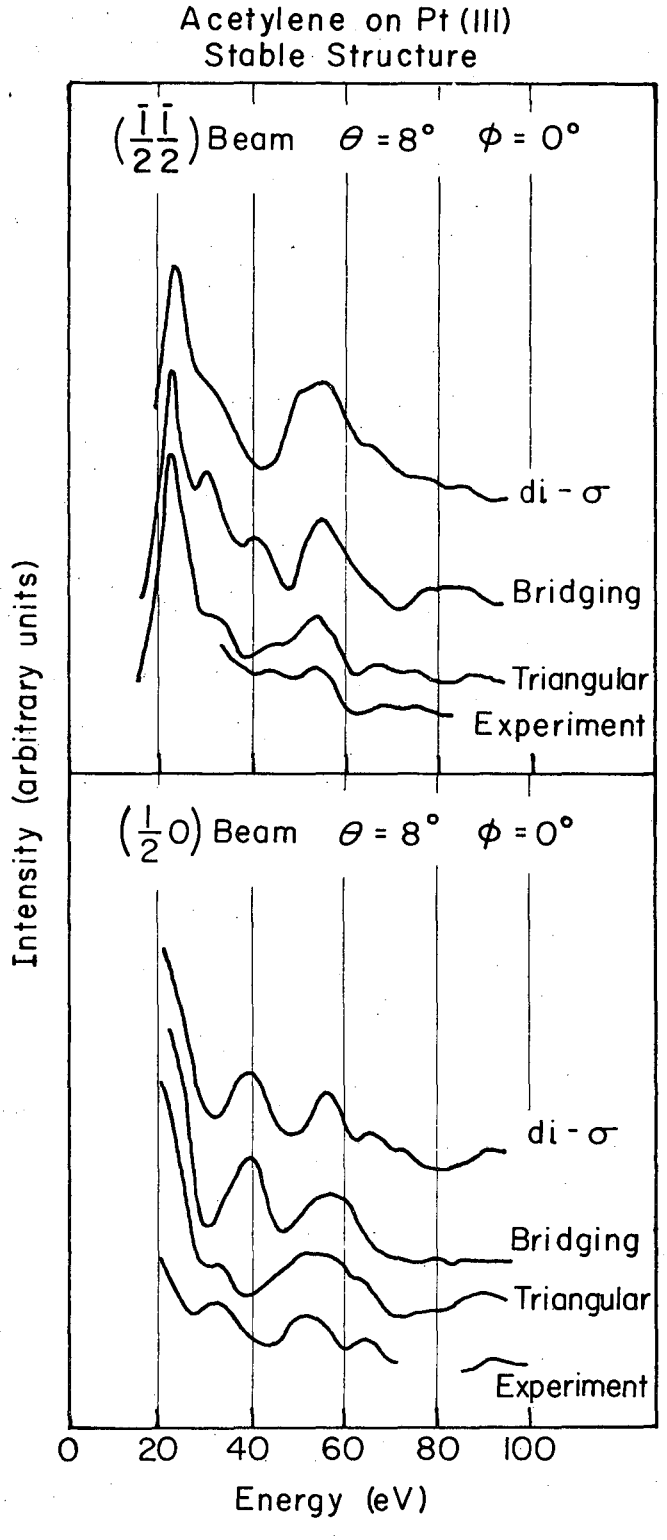

XBL 772-5052

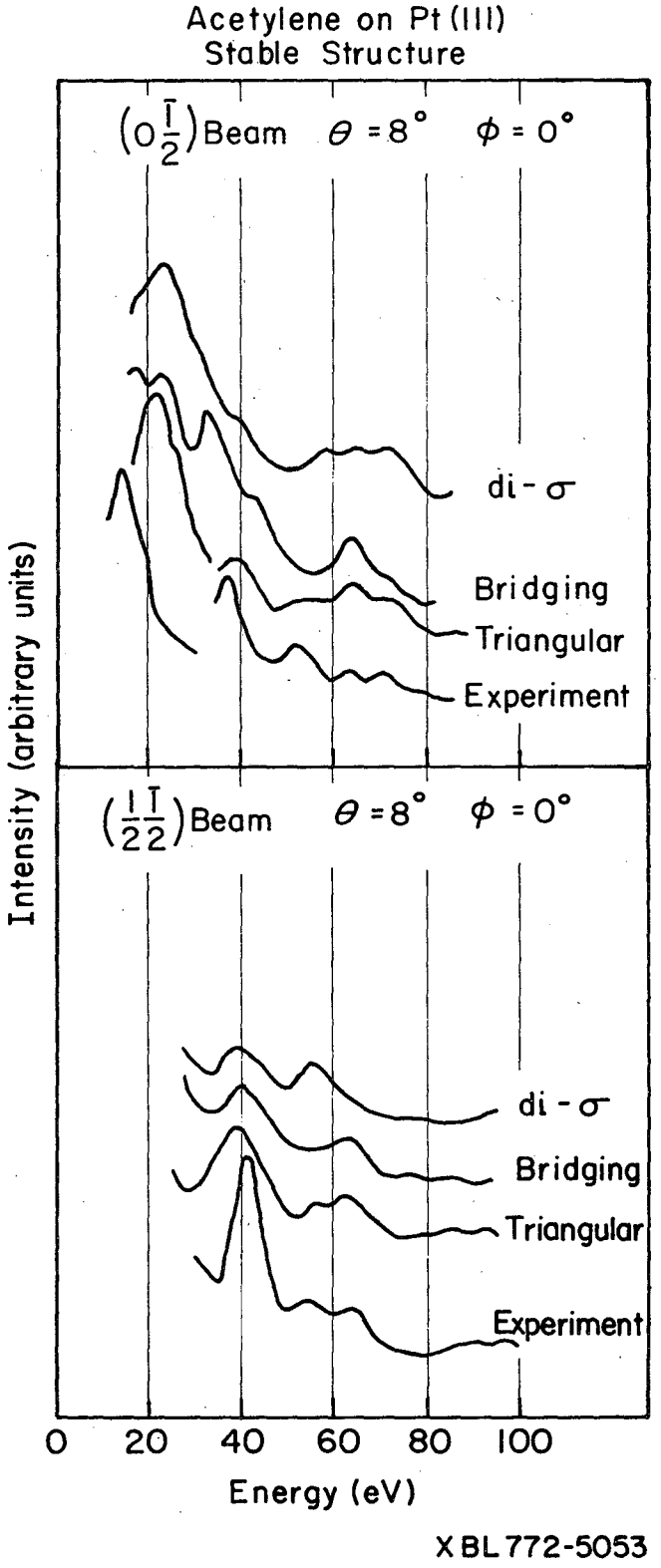
Acetylene on Pt(111)
Stable Structure
$(0\bar{1}/2)$ Beam $\theta = 8°$ $\phi = 0°$
di-σ
Bridging
Triangular
Experiment
$(\frac{1}{2}\bar{1}/2)$ Beam $\theta = 8°$ $\phi = 0°$
di-σ
Bridging
Triangular
Experiment
Intensity (arbitrary units)
0
20
40
60
80
100
Energy (eV)

XBL772-5053

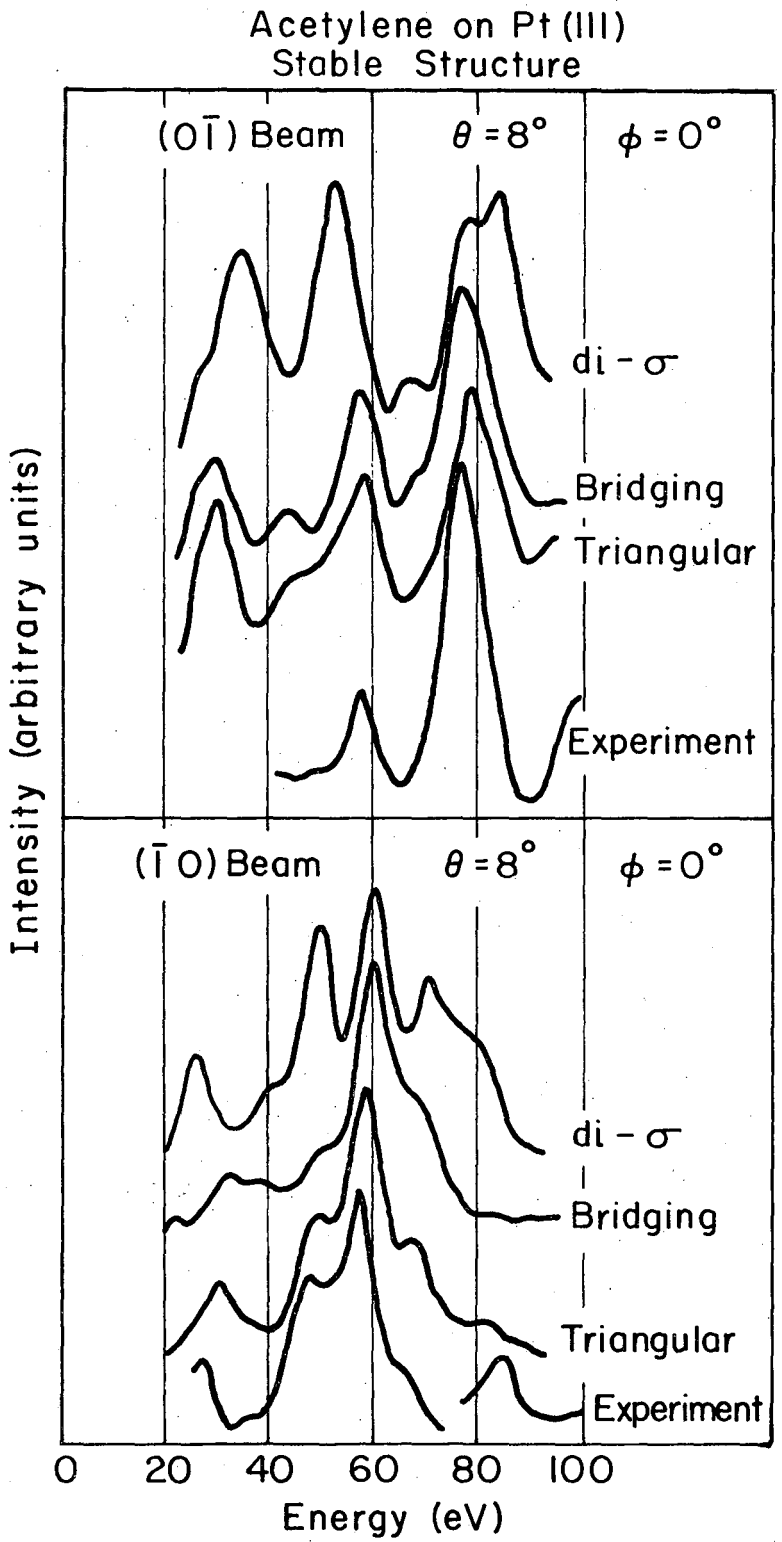

XBL 767-7146

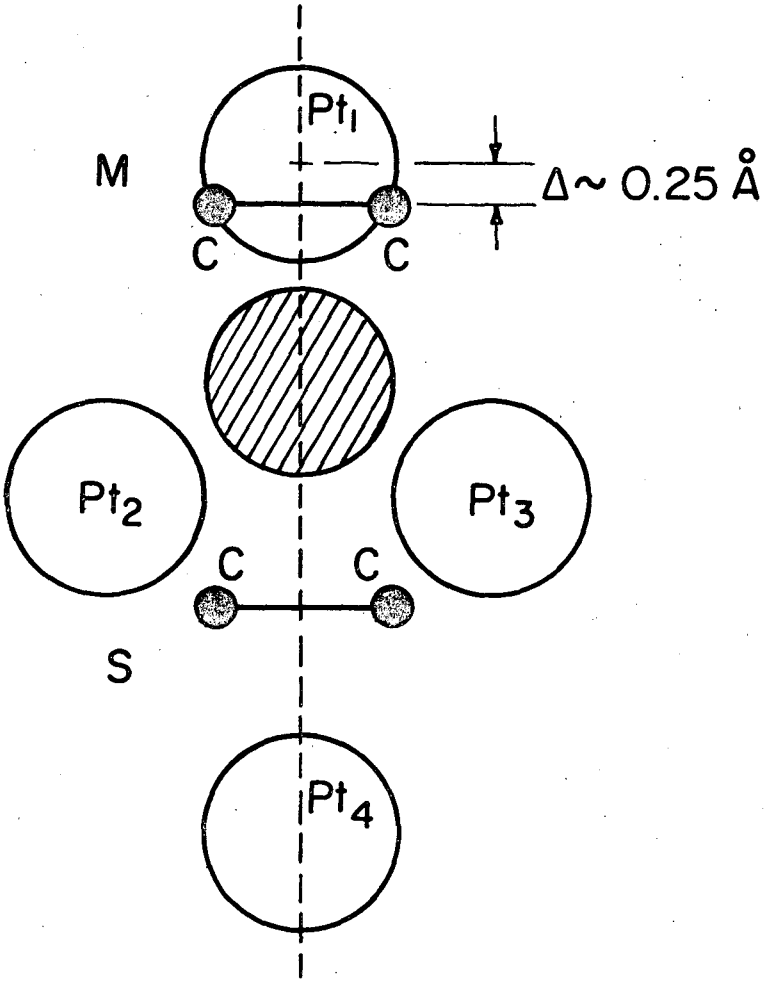

XBL 772-5063

15

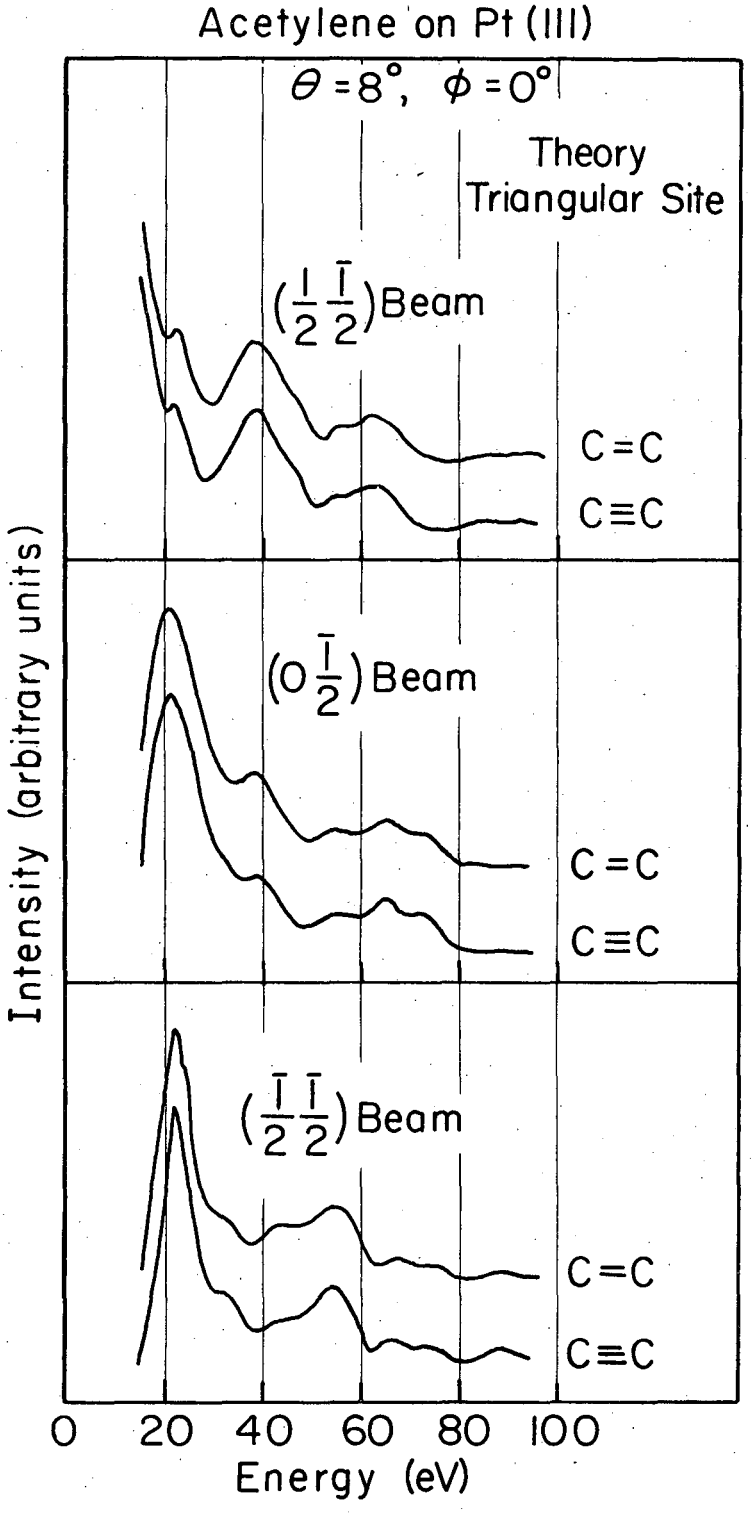

XBL 772-5048

A1

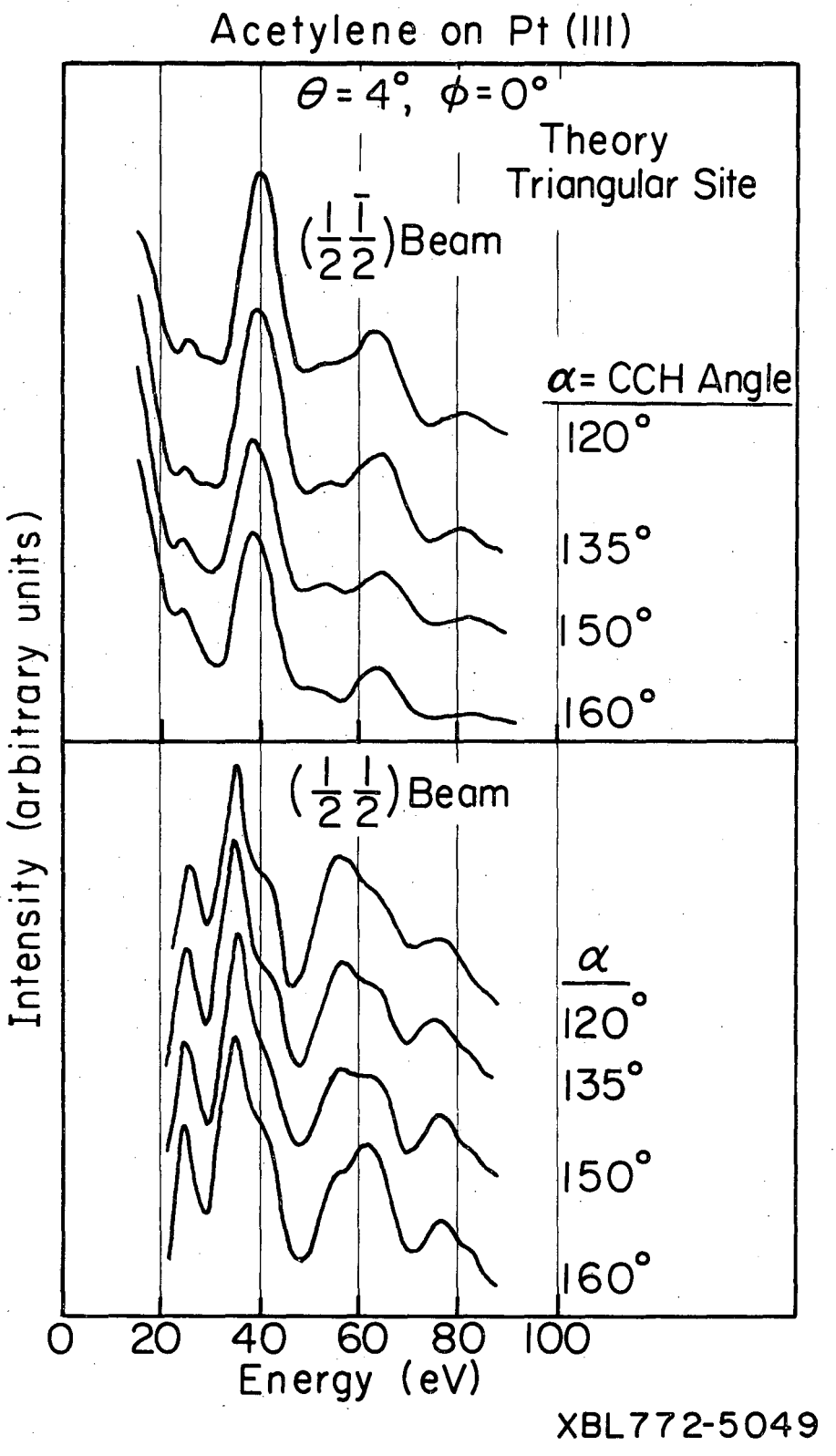
Acetylene on Pt (111)
θ = 4°, φ = 0°
Theory
Triangular Site
(1/2 1̄/2) Beam
α = CCH Angle
120°
135°
150°
160°
(1/2 1/2) Beam
α
120°
135°
150°
160°
Intensity (arbitrary units)
0
20
40
60
80
100
Energy (eV)
XBL772-5049

A2

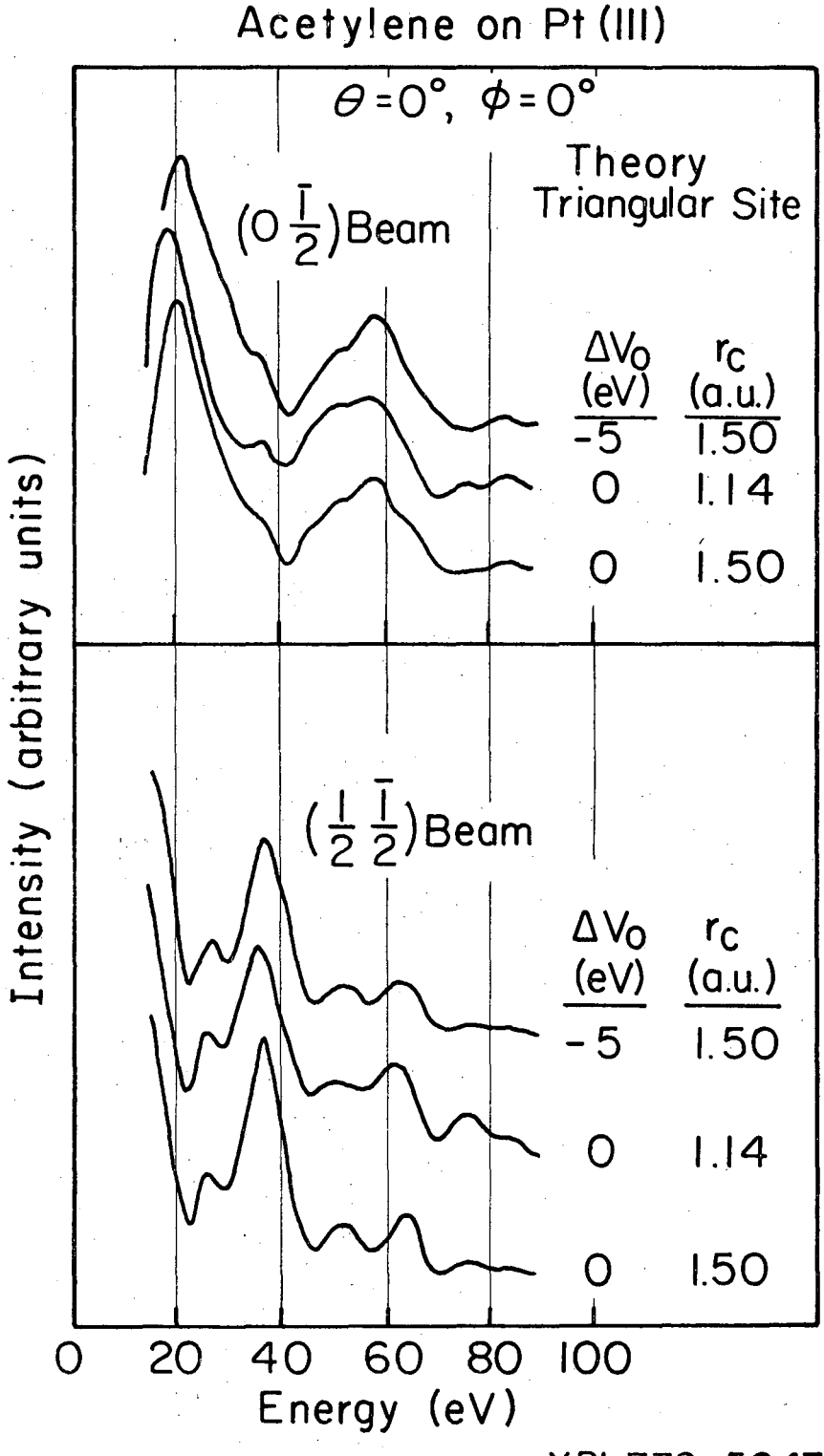

XBL772-5047

A3

TECHNICAL INFORMATION DIVISION
LAWRENCE BERKELEY LABORATORY
UNIVERSITY OF CALIFORNIA
BERKELEY, CALIFORNIA 94720